
Since January 2020 Elsevier has created a COVID-19 resource centre with free information in English and Mandarin on the novel coronavirus COVID-19. The COVID-19 resource centre is hosted on Elsevier Connect, the company's public news and information website.

Bioorg. Med. Chem. 87 (2023) 117316

Contents lists available at ScienceDirect

Bioorganic & Medicinal Chemistry

journal homepage: www.elsevier.com/locate/bmc

# Design, synthesis and biological evaluation of covalent peptidomimetic 3CL protease inhibitors containing nitrile moiety

Mengwei Zhu [a,b,1], Tiantian Fu [a,b,1], Mengyuan You [c,1], Junyuan Cao [d,e,1], Hanxi Yang [f], Xinyao Chen [b,g], Qiumeng Zhang [h], Yechun Xu [c,h], Xiangrui Jiang [h], Leike Zhang [d,e,*], Haixia Su [h,*], Yan Zhang [h,*], Jingshan Shen [h]

[a] College of Pharmacy, An Hui University of Traditional Chinese Medicine, Hefei 230012, China
[b] Yangtze Delta Drug Advanced Research Institute and Yangtze Delta Pharmaceutical College, Nantong 226133, China
[c] School of Chinese Materia Medica, Nanjing University of Chinese Medicine, Nanjing 210023, China
[d] State Key Laboratory of Virology, Wuhan Institute of Virology, Center for Biosafety Mega-Science, Chinese Academy of Sciences, Wuhan, Hubei 430071, China
[e] Hubei Jiangxia Laboratory, Wuhan 430200, China
[f] College of Chemistry, Zhengzhou University, Zhengzhou 450001, China
[g] Wuya College of Innovation, Shenyang Pharmaceutical University, Shenyang 110016, China
[h] State Key Laboratory of Drug Research, Shanghai Institute of Materia Medica, Chinese Academy of Sciences, Shanghai 201203, China

ARTICLE INFO

*Keywords:*
COVID-19
SARS-CoV-2
3CL protease
Nirmatrelvir
Peptidomimetic inhibitors

ABSTRACT

In this paper, a series of peptidomimetic SARS-CoV-2 3CL protease inhibitors with new *P*2 and *P*4 positions were synthesized and evaluated. Among these compounds, **1a** and **2b** exhibited obvious $3CL^{pro}$ inhibitory activities with $IC_{50}$ of 18.06 nM and 22.42 nM, respectively. **1a** and **2b** also showed excellent antiviral activities against SARS-CoV-2 *in vitro* with $EC_{50}$ of 313.0 nM and 170.2 nM, respectively, the antiviral activities of **1a** and **2b** were 2- and 4-fold better than that of nirmatrelvir, respectively. In vitro studies revealed that these two compounds had no significant cytotoxicity. Further metabolic stability tests and pharmacokinetic studies showed that the metabolic stability of **1a** and **2b** in liver microsomes was significantly improved, and **2b** had similar pharmacokinetic parameters to that of nirmatrelvir in mice.

## 1. Introduction

Since late 2019, the outbreak of coronavirus disease 2019 (COVID-19) caused by severe acute respiratory syndrome coronavirus 2 (SARS-CoV-2),[1,2] poses a severe threat to global public health and safety. Although vaccines have been widely and repeatedly vaccinated, the high variability and certain immune escape ability of SARS-CoV-2 makes the vaccines less effective.[3,4] Therefore, the development of antiviral agents that retain activity against various SARS-CoV-2 variants is still necessary to relieve the symptoms and reduce the hospitalization rate of patients.[5]

During the replication of coronaviruses, 3-chymotrypsin-like cysteine protease (3CL protease, $3CL^{pro}$) and papain-like protease ($PL^{pro}$) are responsible for the cleavage of two polyprotein precursors (pp1a/pp1ab) into nonstructural proteins, which are essential for viral genome replication and transcription.[6–9] $3CL^{pro}$ gene sequences are highly conserved among coronaviruses that have been discovered, and have no homologous proteins in humans.[10–12] $3CL^{pro}$ inhibitors can be classified as peptidomimetic and non-peptidomimetics,[13] Peptidomimetic $3CL^{pro}$ inhibitors were designed by mimicking peptide substrates. The active site of $3CL^{pro}$ is highly conserved and usually consists of four subsites: S1′, S1, S2 and S4, which can be occupied by the *P*1′, *P*1, *P*2 and *P*4 portions of peptidomimetic inhibitors.[14,15] The reported chemical warheads of $3CL^{pro}$ inhibitors at the *P*1′ position including nitrile, α,β-unsaturated ester, phthalhydrazido-methyl ketone, benzothiazolyl ketone, aldehyde, α-ketoamide, hydroxymethyl ketone, acrylamide, 2-butynamide and so on.[16,17] According to the specificity and catalytic mechanism of the substrate, the inhibitors can competitively bind $3CL^{pro}$ with the natural substrate, further inactivating $3CL^{pro}$.[18,19] Therefore, $3CL^{pro}$ has become one of the most important targets for anti coronavirus drug research.

* Corresponding authors at: State Key Laboratory of Virology, Wuhan Institute of Virology, Center for Biosafety Mega-Science, Chinese Academy of Sciences, Wuhan, Hubei 430071, China (L. Zhang).
*E-mail addresses:* zhangleike@wh.iov.cn (L. Zhang), suhaixia1@simm.ac.cn (H. Su), zhang_yan@simm.ac.cn (Y. Zhang).
[1] Mengwei Zhu, Tiantian Fu, Mengyuan You and Junyuan Cao contributed equally to this work.

https://doi.org/10.1016/j.bmc.2023.117316
Received 30 March 2023; Received in revised form 27 April 2023; Accepted 3 May 2023
Available online 8 May 2023

Nirmatrelvir, a 3CL$^{pro}$ inhibitor, which is the active pharmaceutical ingredient of Paxlovid approved by the FDA for emergency use in the treatment of COVID-19.[20] Several groups reported similar designs as nirmatrelvir at the same time, and some 3CL$^{pro}$ inhibitors containing dimethylcyclopropylproline or cyclopentylproline at the *P*2 position were synthesized. Kneller et al. reported that BBH-1, BBH-2 and NBH-2 exhibited comparable antiviral properties to that of nirmatrelvir *in vitro* (Fig.1).[21] Xia et al. designed two 3CL$^{pro}$ inhibitors UAWJ9-36-1 and UAWJ9-36-3, which also contain γ-lactam ring at the *P*1 position, exhibited broad-spectrum anti-coronavirus activity (Fig.1).[22] Qiao et al. reported that MI-09 and MI-30 showed excellent antiviral activity in cell-based assays and displayed good pharmacokinetic properties in rats (Fig.1).[23]

In this paper, we designed and synthesized a series of peptidomimetic SARS-CoV-2 3CL$^{pro}$ inhibitors based on the structure of nirmatrelvir, and evaluated their biological activities. Among these compounds, **1a** and **2b** showed excellent inhibitory potency against SARS-CoV-2 3CL$^{pro}$ and notable antiviral activity against SARS-CoV-2 *in vitro*, which provided lead compounds for the development of clinical drug candidates. The design of peptidomimetic SARS-CoV-2 3CL$^{pro}$ inhibitors is shown in Fig.2.

## 2. Results and discussion

### 2.1. Chemistry

The synthetic route of compounds **1 (a–f)** is shown in Scheme 1. The *tert*-Butoxycarbonyl (Boc) group of commercially available **1**–**1 (a–f)** was deprotected and then conjugated with *N*-Boc-L-*tert*-leucine to afford ester **1**–**2 (a–f)**, then **1**–**3 (a–f)** were obained via alkaline hydrolysis. Compound **1**–**4** was prepared according to the method reported in Ref. 24. **1**–**4** was deprotected in the presence of HCl-Dioxane, and then coupled with **1**–**3 (a–f)** using HATU as coupling reagent to generate **1**–**5 (a–f)**. Finally, the Boc group of **1**–**5 (a–f)** was deprotected, and trifluoroacetic anhydride (TFAA) was used to achieve the trifluoroacetylation of amino group and dehydration of amide to nitrile in a one-pot reaction to obtain compounds **1 (a–f)**.

The synthesis of compounds **2 (a–d)** was similar to the above. Removal of the Boc group of **2**–**4** and then reacted with different acid chlorides or anhydrides to give **2**–**5 (a–d)**. Finally, **2**–**5 (a–d)** were dehydrated with Burgess reagent to obtain compounds **2 (a–d)**. (Scheme 2).

### 2.2. Biological assay

The use of nitrile warhead at *P*1′ is one of the key factors contributing to the excellent activity of nirmatrelvir. The nitrile warhead can react with the sulfhydryl group of the cysteine 145 residue at S1′ site to form a reversible covalent thioimidate adduct, which is important for the inhibitors to maintain antiviral activity.[25] The S1 site of 3CL$^{pro}$ has an extremely high recognition specificity for glutamine residues, and nirmatrelvir adopts the γ-lactam ring as the *P*1 fragment. γ-lactam ring has the ability to mimic glutamine, it can penetrate into the S1 site and form a stable interaction with the residues at S1 site.[26] Several groups reported that boceprevir had potent SARS-CoV-2 3CL$^{pro}$ inhibitory activity as well as cellular antiviral activity.[27,28] And X-ray crystal structure analysis revealed that the binding of boceprevir to the catalytically active side of SARS-CoV-2 3CL$^{pro}$ is the main mechanism of inhibition.[29,30] These results demonstrated that the dimethylcyclopropylproline of boceprevir has an important effect on antiviral activity, which provided the guidance for the design of new 3CL$^{pro}$ inhibitors.

Based on this, we firstly modified the *P*2 position of nirmatrelvir. In order to investigate the importance of bicyclic proline, a series of compounds with different bicyclic proline at *P*2 position were synthesized and evaluated (Table 1). The compound **1a**, bearing cyclopentyl proline, displayed a similar inhibitory potency to that of nirmatrelvir at 0.1 μM (**1a** inhibition was 82.50%, Nirmatrelvir inhibition was 91.38%). **1b** and **1c**, bearing bridged bicyclic proline and spiro bicyclic proline, exhibited slightly lower inhibitory potency than that of **1a** at 0.1 μM (**1b** inhibition was 47.38%, **1c** inhibition was 54.47%). This indicated that cyclopentyl

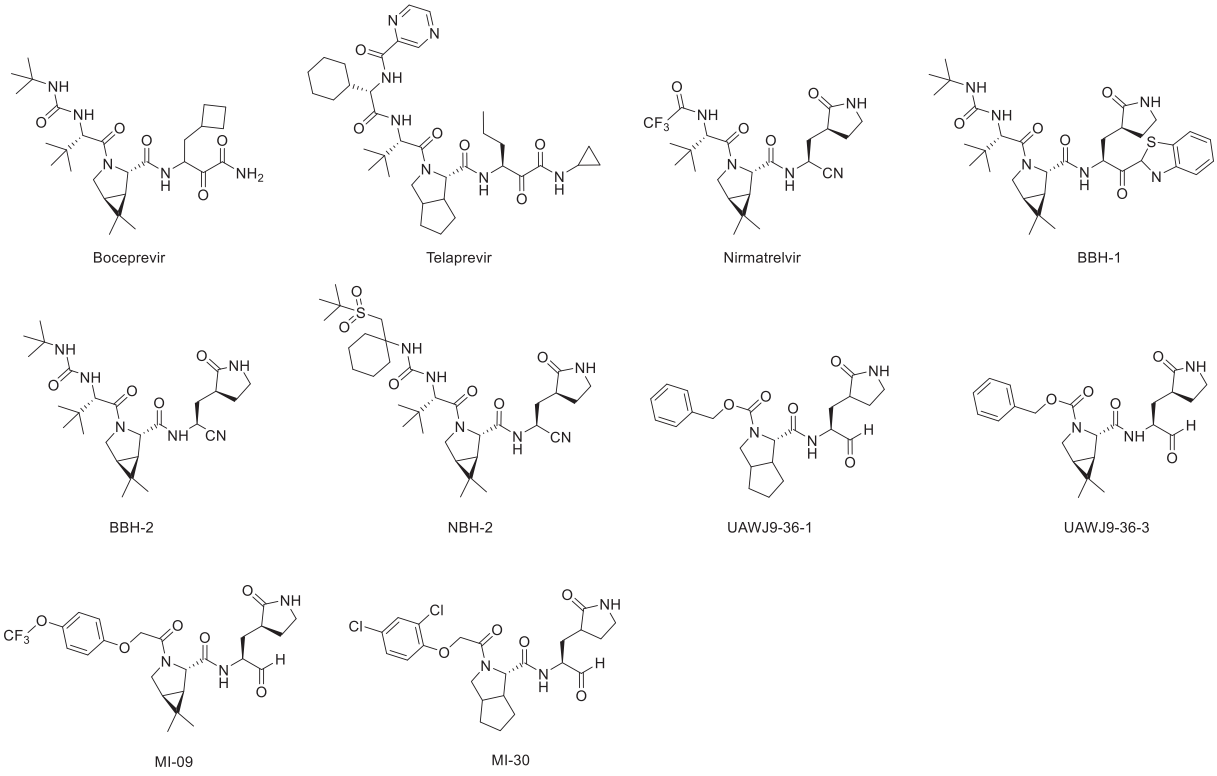


**Fig. 1.** Chemical structures of protease inhibitors.

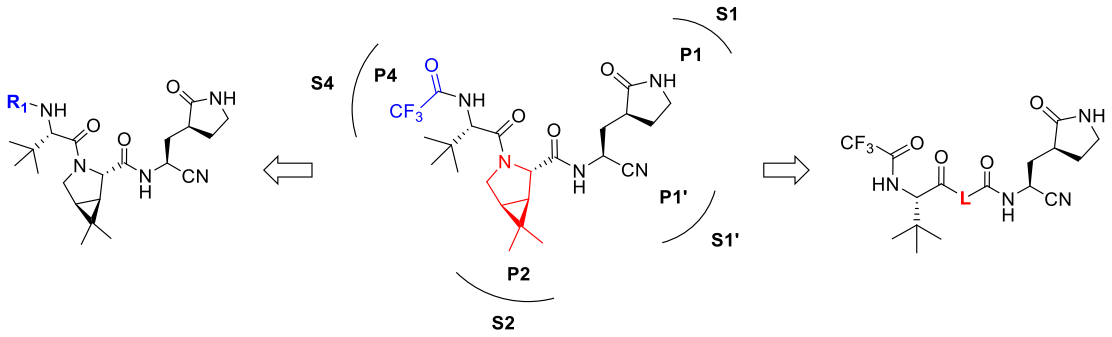


**Fig. 2.** Design of peptidomimetic SARS-CoV-2 $3CL^{pro}$ inhibitors.

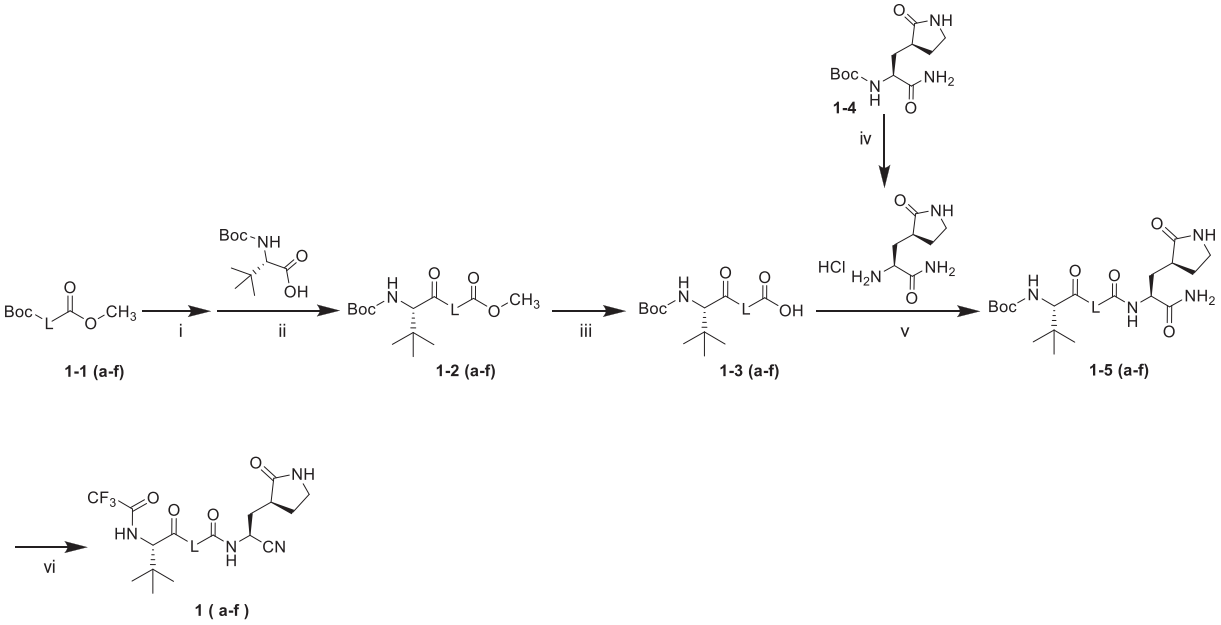


**Scheme 1.** Synthesis of compounds **1 (a–f)**, reagents and conditions: (i) 4 N HCl-Dioxane, Dioxane, 40 ℃, 1 h; (ii) BOP, NMM, *N,N*-Dimethylformamide, DCM, 25 ℃, 10 h; (iii) $LiOH{\cdot}H_2O$, THF, $H_2O$, 40 ℃, 2 h; (iv) 4 N HCl-Dioxane, Dioxane, 40 ℃, 1 h; (v) HATU, DIPEA, DCM, 25 ℃, 10 h; (vi) 4 N HCl-Dioxane, Dioxane, 40 ℃, 1 h; TFAA, $Et_3N$, 25 ℃, 10 h.

proline was more easily bound to the S2 pocket of $3CL^{pro}$.

In the published $3CL^{pro}$ inhibitors, isobutyl group was mostly adopted at *P*2 position.[31–33] We speculate that the size and flexible conformation of the substituents at *P*2 position may influence their binding to S2 pocket. Therefore, isobutyl group and cyclopropyl vinyl group were introduced at the α-C of nitrogen atom (Table 1). The inhibitory activities of compound **1d** (isobutyl group) and **1f** (cyclopropyl vinyl group) were severely reduced compared to that of nirmatrelvir. In addition, compound **1e** bearing hydrophilic morpholine at the *P*2 position showed poor inhibitory potency (10 μM inhibition was 49.05%, Table 1). This result was consistent with our prediction, indicating that polarity of substituents at *P*2 position had an important influence on the inhibitor activity.[34]

Generally, S4 pocket has a low specificity for the substrate, while *P*4 position may affect the metabolic stability of the inhibitors.[35,36] So, we replaced the *P*4 position with different groups in order to screen compounds with better biological activities. Firstly, we synthesized compound **2a** by introducing pentafluoropropionyl at the *P*4 position of nirmatrelvir (Entry 7, Table 1). Unfortunately, The inhibitory activity of compound **2a** was greatly reduced at low concentrations. A previous report revealed that the introduction of halogenated phenyl rings at the *P*4 position were able to form hydrophobic interactions with the S4 site.[23] Inspired by this, we synthesized compound **2d** by introducing a 3,5-bis (trifluoromethyl) phenyl group at the *P*4 position, however, the result showed **2d** had a low inhibitory activity (Entry 10, Table 1).

According to the report, methanesulfonyl group at the *P*4 position can extend underneath $Gln^{189}$ to improve the hydrogen bonding interactions. The introduction of the methanesulfonyl group was also able to improve the antiviral activity, human liver microsomal stability and oral absorption of the inhibitor.[24] We introduced trifluoromethanesulfonyl and cyclopropylsulfonyl at the *P*4 position to synthesize compounds **2b** and **2c** (Table 1). The results showed that **2b** and **2c** had similar inhibitory activities to that of nirmatrelvir, the inhibition at 0.1 μM was 95.33% and 94.94%, respectively (Entry 8 and 9, Table 1). This indicates that sulfonyl group plays an important impact on the inhibitory activity.

The preliminary screening results showed that compounds **1a**, **1b**, **1c**, **2b** and **2c** had good inhibitory activities against $3CL^{pro}$, we further tested $IC_{50}$ and RNA copy inhibition of these compounds. The results showed that the $IC_{50}$ of these five compounds were slightly better than that of nirmatrelvir (Table 1). The preliminary screening results showed that the RNA copy inhibition of **1a** and **2b** reached 70% and 98% at 1 μM. Therefore, we selected **1a** and **2b** for further research based on the above data.

We studied the cytotoxicity of **1a** and **2b** in Vero E6 cells, neither of the two compounds showed obvious cytotoxicity (Entry 1 and 8,

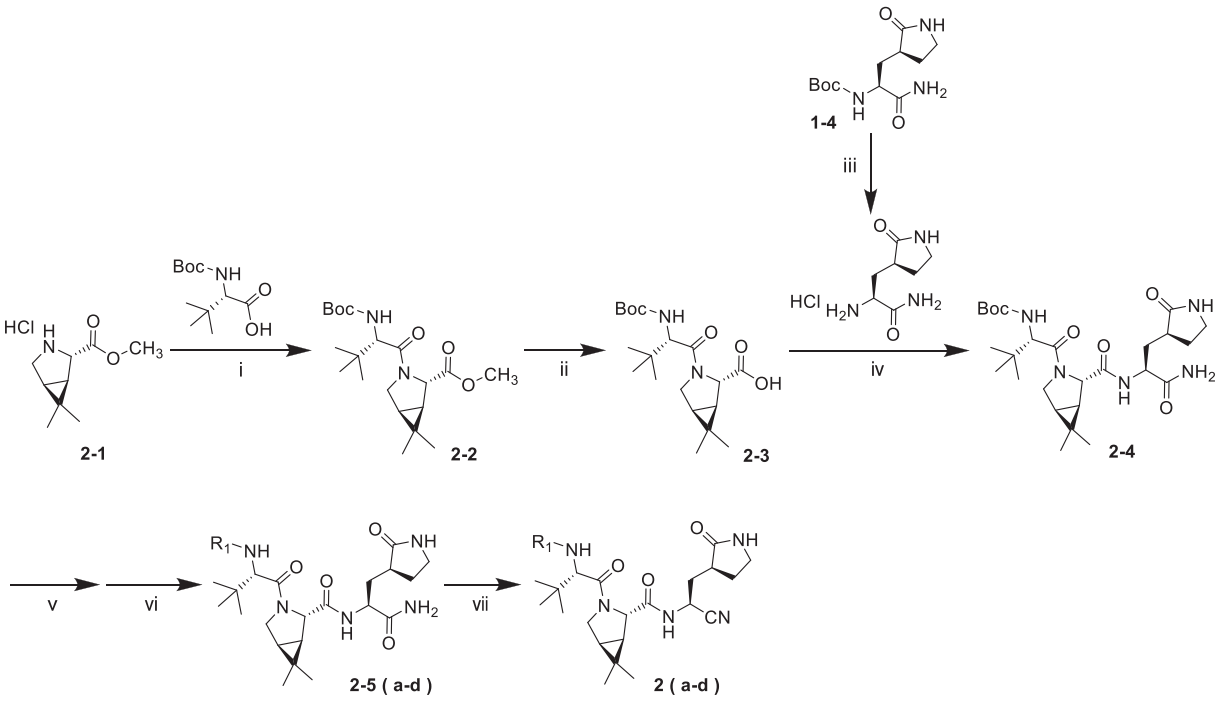


**Scheme 2.** Synthesis of compounds **2 (a–d)**, reagents and conditions: (i) BOP, NMM, *N,N*- Dimethylformamide, DCM, 25 ℃, 10 h; (ii) LiOH·$H_2O$, THF, $H_2O$, 40 ℃, 2 h; (iii) 4 N HCl-Dioxane, Dioxane, 40 ℃, 1 h; (iv) HATU, DIPEA, DCM, 25 ℃, 10 h; (v) 4 N HCl-Dioxane, Dioxane, 40 ℃, 1 h; (vi) $Et_3N$, DCM, 0 ℃, 10 h; (vii) Burgess Reagent, DCM, 25 ℃, 10 h.

Table 1). Subsequently, we tested the $EC_{50}$ of these two compounds. The results showed that the $EC_{50}$ of the two compounds were 313.0 nM and 170.2 nM, respectively, indicating that the antiviral activities were 2- and 4-fold that of nirmatrelvir (Table 1).

In addition, we studied the metabolic stability of **1a** and **2b** in human liver microsomes and mouse liver microsomes (Table 2). **1a** showed moderate metabolic stability in human liver microsomes, but was susceptible to metabolic effects in mouse liver microsomes. **2b** was stable in human liver microsomes, and also showed moderate metabolic stability in mouse liver microsomes. Compared with nirmatrelvir, the metabolic stability of these two compounds has been significantly improved. These results were consistent with our prediction, indicating that the introduction of sulfonyl group at *P4* position can improve the metabolic stability of inhibitors.

Finally, we conducted pharmacokinetic (PK) studies on **1a** and **2b** *in vivo*. The two compounds showed favorable pharmacokinetic properties, with oral bioavailability of 22.80% and 23.09%, respectively (Table 3). When administered intravenously (i.v.) (10 mg/kg) and orally (p.o.) (20 mg/kg), **1a** showed area under the curve (AUC) values of 2669 h*ng/mL and 1219 h*ng/mL, respectively, whereas **2b** displayed AUC values of 4118.55 h*ng/mL and 1901.84 h*ng/mL, respectively. After p.o. administration, **1a** showed peak blood concentration ($C_{max}$) values of 1311 ng/mL, **2b** displayed $C_{max}$ values of 2052.36 ng/mL. This series of pharmacokinetic parameters showed that **2b** had similar $C_{max}$ and $AUC_{last}$ to nirmatrelvir, which indicated that it have the potential to develop into an oral drug.

## 3. Conclusion

As the COVID-19 pandemic and the constant variation of the virus, the development of drugs against SARS-CoV-2 is still of great significance. Based on the structure of nirmatrelvir, we synthesized a series of peptidomimetic SARS-CoV-2 $3CL^{pro}$ inhibitors and tested their biological activities. Among these inhibitors, **1a** and **2b** exhibited excellent enzyme inhibitory potency with $IC_{50}$ of 18.06 nM and 22.42 nM, respectively. **1a** and **2b** also showed significant antiviral activities against SARS-CoV-2 *in vitro* with $EC_{50}$ of 313.0 nM and 170.2 nM, respectively. The results of liver microsome stability tests showed that the metabolic stability of **1a** and **2b** was significantly improved compared to nirmatrelvir, **2b** also showed similar pharmacokinetic properties to nirmatrelvir. All such results suggested **1a** and **2b** deserved further evaluation, and provided important clues for further optimization.

## 4. Experimental

### 4.1. Materials and methods

All commercially available chemicals and solvents were directly used without further purification. All reactions were monitored by thin layer chromatography (TLC) on silica gel plates (GF-254). High-resolution mass spectra (HRMS) were measured on an Agilent 1290–6545 UHPLC-QTOF LC/MS spectrometer. $^1H$ NMR and $^{13}C$ NMR data were recorded on a Bruker AVANCE III instrument (400 MHz) using TMS as an internal standard. Molecular mass was determined on a mass spectrometry (Waters (China) Co., Ltd.). All tested compounds exhibited purities of >95% as analyzed by HPLC (Dionex UltiMate 3000, Germany).

### 4.2. Synthetic procedures

#### 4.2.1. Synthesis of ethyl(1S,3aR,6aS)-2-((S)-2-((tert-butoxycarbonyl) amino)-3,3-dimethylbutanoyl) octahydrocyclopenta[c]pyrrole-1-carboxylate (1-2a)

(S)-2-((*tert*-butoxycarbonyl)amino)-3,3-dimethylbutanoic acid (1.0 g, 4.3 mmol) and ethyl (1S,3aR,6aS)-octahydrocyclopenta[*c*]pyrrole-1-carboxylate **1-1a** (1.0 g, 4.8 mmol) were dissolved in DCM/DMF (V:V = 1:1, 20 mL) solution. Then 4-Methylmorpholine (1.3 g, 13.0 mmol), BOP (2.3 g, 5.2 mmol) were added to the reaction at 25 °C and stirred for 10 h. Then DCM (70 mL) and 1 N HCl aqueous solution (8 mL) were added to the reaction. After separation, the organic phase was washed with $H_2O$ (10 mL), the organic phase was washed with saturated brine (10

**Table 1**
The inhibitory activity, anti-viral potency and cytotoxicity against SARS-CoV-2 3CL$^{pro}$ of inhibitors.

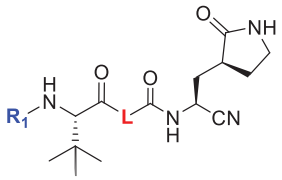

| Entry | Cmpd. | $R_1$ | L | SARS-CoV-2 3CL$^{pro}$ Inhibition (%), μM | | | | $IC_{50}$ nM | $EC_{50}$ nM | $CC_{50}$ μM | SI |
|---|---|---|---|---|---|---|---|---|---|---|---|
| | | | | 0.02 | 0.1 | 1 | 10 | | | | |
| 1 | **1a** | 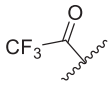 | 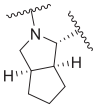 | 23.99 | 82.50 | 88.88 | 88.30 | 18.06 ± 2.35 | 313.0 ± 63.6 | > 200 | > 600 |
| 2 | **1b** | 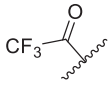 | 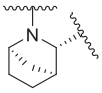 | / | 47.38 | 92.62 | 97.13 | 54.64 ± 12.98 | / | / | / |
| 3 | **1c** | 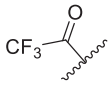 | 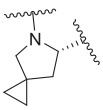 | / | 54.47 | 95.83 | 96.99 | 36.82 ± 1.99 | / | / | / |
| 4 | **1d** | 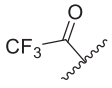 | 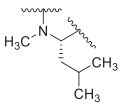 | / | / | 54.69 | 80.03 | / | / | / | / |
| 5 | **1e** | 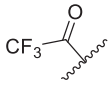 | 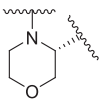 | / | / | / | 49.05 | / | / | / | / |
| 6 | **1f** | 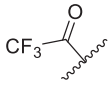 | 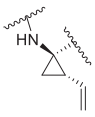 | / | / | / | 25.25 | / | / | / | / |
| 7 | **2a** | 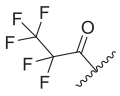 | 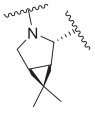 | / | −4.36 | 95.19 | 99.91 | / | / | / | / |
| 8 | **2b** | 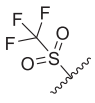 | 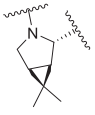 | 18.04 | 95.33 | 106.86 | 95.22 | 22.42 ± 2.78 | 170.2 ± 84.4 | > 200 | > 1500 |
| 9 | **2c** | 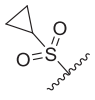 |  | 46.94 | 94.94 | 108.66 | 111.68 | 22.83 ± 0.21 | / | / | / |
| 10 | **2d** | 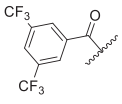 |  | / | / | / | 52.49 | / | / | / | / |
| 11 | Nirmatrelvir* | 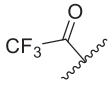 | 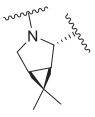 | 41.64 | 91.38 | 92.38 | 88.59 | 41.65 ± 2.37 | 579.5 ± 74.5 | / | / |

Note:/:No test.
*:reported compound.
$IC_{50}$ and $EC_{50}$ values are shown as means ± SD (n = 3).
The antiviral activity of tested compounds against the original SARS-CoV-2 stain in Vero E6 cells.

mL), dried over anhydrous sodium sulphate, evaporated in vacuum and purified by column chromatography (silica gel, PE/EA = 20/1–8/1) to give the compound **1-2a**. Yield 51.8%; colourless oil; $^1$H NMR (400 MHz, DMSO-$d_6$) $\delta$ 6.61 (d, $J$ = 9.1 Hz, 1H), 4.14 (q, $J$ = 4.2, 3.2 Hz, 2H), 4.09 (d, $J$ = 7.1 Hz, 1H), 4.07–4.02 (m, 1H), 3.74 (qd, $J$ = 10.3, 5.1 Hz, 2H), 2.76–2.65 (m, 1H), 2.58 (tt, $J$ = 7.9, 4.1 Hz, 1H), 1.91–1.73 (m, 2H), 1.64 (dt, $J$ = 14.5, 5.6 Hz, 1H), 1.59–1.49 (m, 2H), 1.48–1.38 (m, 1H), 1.37 (s, 9H), 1.17 (t, $J$ = 7.1 Hz, 3H), 0.94 (s, 9H). $^{13}$C NMR (101 MHz, DMSO-$d_6$) $\delta$ 172.07, 170.62, 156.25, 78.66, 65.18, 60.84, 58.66, 53.67, 47.23, 43.16, 34.80, 32.63, 31.71, 28.57, 26.75, 25.09, 14.50. ESI-MS $m/z$ 397.23 $[M + H]^+$.

**Table 2**
Liver microsomal stability of **1a** and **2b**.

| Entry | Cmpd. | Liver microsomes | $T_{1/2}$ (minute) | Clint (mL/min/kg) |
|---|---|---|---|---|
| 1 | **1a** | HUMAN | 78.89 | 22.03 |
| | | MOUSE | 14.85 | 367.52 |
| 2 | **2b** | HUMAN | 652.17 | 2.67 |
| | | MOUSE | 97.89 | 55.75 |
| 3 | Nirmatrelvir | HUMAN | 37.93 | 45.83 |
| | | MOUSE | 4.64 | 1175.45 |

Note:human, mouse liver microsomes from Xenotech.

#### *4.2.2. Synthesis of (1S,3aR,6aS)-2-((S)-2-((tert-butoxycarbonyl)amino)-3,3-dimethylbutanoyl) octahydrocyclopenta[c]pyrrole-1-carboxylic acid (**1-3a**)*

Compound **1-2a** (460 mg, 1.2 mmol), lithium hydroxide (201 mg, 4.8 mmol) and water (5 mL) were dissolved in THF (5 mL) solution at 40 °C and stirred for 2 h. Then 1 N HCl aqueous solution was added to the reaction to adjust the pH 2–3. EA (40 mL) was added to the solution and separation, the organic phase was washed with saturated brine (10 mL), dried over anhydrous sodium sulphate, evaporated in vacuum and purified by column chromatography (silica gel, DCM/MeOH = 80/1–20/1) to give the compound **1-3a**. Yield 99.2%; white solid; $^1$H NMR (400 MHz, DMSO-$d_6$) $\delta$ 12.35 (s, 1H), 6.58 (d, $J$ = 9.2 Hz, 1H), 4.17–4.12 (m, 1H), 4.10 (d, $J$ = 4.1 Hz, 1H), 3.73 (qd, $J$ = 10.2, 4.8 Hz, 2H), 2.72–2.63 (m, 1H), 2.59 (tt, $J$ = 7.8, 4.0 Hz, 1H), 1.90–1.83 (m, 2H), 1.78 (p, $J$ = 7.2 Hz, 1H), 1.69–1.59 (m, 1H), 1.54 (dq, $J$ = 8.2, 5.3, 4.3 Hz, 2H), 1.38 (s, 9H), 0.95 (s, 9H). $^{13}$C NMR (101 MHz, DMSO-$d_6$) $\delta$ 173.63, 172.41, 156.25, 78.63, 65.13, 58.60, 53.71, 47.27, 43.09, 34.85, 32.91, 31.87, 28.57, 26.78, 25.16. ESI-MS $m/z$ 369.07 $[M + H]^+$.

#### *4.2.3. Synthesis of tert-butyl((S)-1-((1S,3aR,6aS)-1-(((S)-1-amino-1-oxo-3-((S)-2-oxopyrrolidin-3-yl)propan-2-yl)carbamoyl)hexahydrocyclopenta[c]pyrrol-2(1H)-yl)-3,3-dimethyl-1-oxobutan-2-yl)carbamate (**1-5a**)*

Compound **1**–**4** (298 mg, 1.1 mmol) and 4 N HCl in 1,4-dioxane (3 mL) were dissolved in DCM (6 mL), the reaction was stirred at 40 °C for 1 h. The reaction was concentrated to remove the solvent and dry HCl salt was obtained. Meanwhile, compound **1-3a** (405 mg, 1.1 mmol) and HATU (646 mg, 1.7 mmol) were dissolved in DCM (8 mL), the reaction was stirred at 25 °C for 30 min. Then *N, N*-Diisopropylethylamine (310 mg, 2.4 mmol) and HCl salt were added to the reaction, the reaction was stirred at 25 °C for 10 h. Then DCM (30 mL) and 1 N HCl aqueous solution (3 mL) were added to the reaction. After separation, the organic phase was washed with $H_2O$ (5 mL), the organic phase was washed with saturated brine (5 mL), dried over anhydrous sodium sulphate, evaporated in vacuum and purified by column chromatography (silica gel, DCM/MeOH = 150/1–20/1) to give the compound **1-5a**. Yield 62.2%; white solid; $^1$H NMR (400 MHz, DMSO-$d_6$) $\delta$ 8.13 (d, $J$ = 8.7 Hz, 1H), 7.54 (s, 1H), 7.21 (s, 1H), 7.01 (s, 1H), 6.58 (d, $J$ = 9.1 Hz, 1H), 4.25 (ddd, $J$ = 12.3, 8.7, 3.6 Hz, 1H), 4.15 (d, $J$ = 4.4 Hz, 1H), 4.13–4.08 (m, 1H), 3.75 (d, $J$ = 8.2 Hz, 1H), 3.68 (d, $J$ = 11.4 Hz, 1H), 3.12 (t, $J$ = 9.0 Hz, 1H), 3.08–2.98 (m, 1H), 2.72–2.60 (m, 1H), 2.45–2.34 (m, 1H), 2.14 (dt, $J$ = 14.1, 8.0 Hz, 1H), 1.96 (dd, $J$ = 15.2, 11.9 Hz, 1H), 1.79 (d, $J$ = 7.0 Hz, 1H), 1.77 (s, 2H), 1.76 (d, $J$ = 6.7 Hz, 1H), 1.69–1.62 (m, 3H), 1.60 (d, $J$ = 12.4 Hz, 2H), 1.36 (s, 9H), 0.92 (s, 9H). $^{13}$C NMR (101 MHz, DMSO-$d_6$) $\delta$ 179.14, 174.02, 172.18, 170.40, 156.27, 78.55, 66.05, 58.79, 54.25, 50.88, 47.63, 43.24, 37.83, 34.83, 34.48, 32.09, 31.64, 28.59, 27.96, 26.84, 24.97. ESI-MS $m/z$ 522.56 $[M + H]^+$.

#### *4.2.4. Synthesis of (1S,3aR,6aS)-N-((S)-1-cyano-2-((S)-2-oxopyrrolidin-3-yl)ethyl)-2-((S)-3,3-dimethyl-2-(2,2,2-trifluoroacetamido)butanoyl) octahydrocyclopenta[c]pyrrole-1-carboxamide (**1a**)*

Compound **1-5a** (104 mg, 0.2 mmol) and TFA (1 mL) were dissolved in DCM (3 mL), the reaction was stirred at 25 °C for 2 h. The reaction was concentrated to remove the solvent. Then triethylamine (73 mg, 0.7 mmol), TFAA (93 mg, 0.4 mmol) and DCM (4 mL) were added to the reaction at 0 °C. The reaction was allowed to warm to 25 °C, and stirred for 10 h. Then DCM (10 mL) and 1 N HCl aqueous solution (2 mL) were added to the reaction. After separation, the organic phase was washed with $H_2O$ (2 mL), the organic phase was washed with saturated brine (2 mL), dried over anhydrous sodium sulphate, evaporated in vacuum and purified by column chromatography (silica gel, DCM/MeOH = 100/1–25/1) to give the compound **1a**. Yield 51.4%; white solid; $^1$H NMR (400 MHz, DMSO-$d_6$) $\delta$ 9.33 (d, $J$ = 8.3 Hz, 1H), 8.92 (d, $J$ = 8.6 Hz, 1H), 7.66 (s, 1H), 4.96 (ddd, $J$ = 11.0, 8.6, 4.9 Hz, 1H), 4.54–4.49 (m, 1H), 4.03 (d, $J$ = 5.0 Hz, 1H), 3.83 (dd, $J$ = 10.4, 7.3 Hz, 1H), 3.63 (dd, $J$ = 10.5, 3.3 Hz, 1H), 3.14 (tt, $J$ = 9.2, 2.0 Hz, 1H), 3.04 (tdd, $J$ = 9.2, 7.1, 1.5 Hz, 1H), 2.77–2.64 (m, 1H), 2.42 (ddd, $J$ = 12.7, 7.3, 3.4 Hz, 1H), 2.21–2.15 (m, 1H), 2.14–2.10 (m, 1H), 2.10–2.05 (m, 1H), 1.84 (dd, $J$ = 7.8, 4.8 Hz, 1H), 1.82–1.80 (m, 1H), 1.80–1.75 (m, 1H), 1.75–1.71 (m, 1H), 1.69 (q, $J$ = 4.6, 3.9 Hz, 1H), 1.67–1.63 (m, 1H), 1.62–1.54 (m, 1H), 1.40–1.31 (m, 1H), 0.98 (s, 9H). $^{13}$C NMR (101 MHz, DMSO-$d_6$) $\delta$ 178.04, 172.12, 168.29, 157.12, 117.75, 114.89, 66.11, 58.46, 54.39, 47.86, 43.51, 38.12, 38.03, 37.18, 35.31, 34.72, 31.81, 31.43, 27.33, 26.69, 25.04. ESI-HRMS Calcd for $C_{23}H_{31}F_3N_5O_4$ $[M-H]^-$: 498.2334, found 498.2334. HPLC: t = 9.335 min, 99.6% purity.

#### *4.2.5. Synthesis of methyl(1R,3S,4S)-2-((S)-2-((tert-butoxycarbonyl)amino)-3,3-dimethylbutanoyl)-2-azabicyclo[2.2.1]heptane-3-carboxylate (**1-2b**)*

Compound **1-2b** was synthesized from compound **1-1b** with *N*-Boc-*L*-*tert*-leucine using methods similar to the method described for the preparation of **1-2a**. Yield 42.9%; white solid; $^1$H NMR (400 MHz, DMSO-$d_6$) $\delta$ 6.42 (d, $J$ = 9.3 Hz, 1H), 4.55 (s, 1H), 4.24–4.18 (m, 1H), 3.87 (s, 1H), 3.61 (s, 3H), 2.61 (s, 1H), 1.85–1.78 (m, 1H), 1.74–1.68 (m, 1H), 1.67 (d, $J$ = 4.4 Hz, 1H), 1.63 (s, 1H), 1.54–1.43 (m, 2H), 1.37 (s, 9H), 0.95 (s, 9H). $^{13}$C NMR (101 MHz, DMSO-$d_6$) $\delta$ 170.71, 168.84, 155.86, 78.60, 63.67, 58.78, 58.49, 52.13, 41.16, 35.57, 35.11, 31.23, 28.61, 27.56, 26.64. ESI-MS $m/z$ 369.24 $[M + H]^+$.

#### *4.2.6. Synthesis of (1R,3S,4S)-2-((S)-2-((tert-butoxycarbonyl)amino)-3,3-dimethylbutanoyl)-2-azabicyclo[2.2.1]heptane-3-carboxylic acid (**1-3b**)*

The compound **1-3b** was synthesized from **1 to 2b** using a procedure similar to that described for the preparation of **1-3a**. Yield 98.0%; white

**Table 3**
Pharmacokinetics parameters of **1a** and **2b** after p.o and i.v. administration in mouse.

| Entry | Cmpd. | $T_{1/2}$ | $T_{max}$ | $C_{max}$ | $AUC_{last}$ | $AUC_{INF\_obs}$ | $CL\_obs$ | $MRT_{INF\_obs}$ | $Vss\_obs$ | F |
|---|---|---|---|---|---|---|---|---|---|---|
| | | (h) | (h) | (ng/mL) | (h*ng/mL) | (h*ng/mL) | (mL/min/kg) | (h) | (mL/kg) | (%) |
| 1 | **1a** (p.o.) | 1.00 | 0.42 | 1311.00 | 1219.00 | 1222.00 | / | 0.88 | / | 22.80 |
| | **1a** (i.v.) | 1.10 | / | / | 2669.00 | 2672.00 | 69.30 | 0.24 | 1011.00 | / |
| 2 | **2b** (p.o.) | 0.71 | 0.50 | 2052.36 | 1901.84 | 1904.90 | / | 0.80 | / | 23.09 |
| | **2b** (i.v.) | 0.35 | 0.08 | 10487.87 | 4118.55 | 4120.05 | 40.95 | 0.29 | 690.00 | / |
| 3 | nirmatrelvir(p.o.) | 0.61 | 0.25 | 2521.64 | 2308.32 | 2311.94 | / | 0.85 | / | 34.59 |
| | nirmatrelvir (i.v.) | 2.83 | 0.083 | 9626.87 | 3336.46 | 3361.32 | 50.06 | 0.39 | 1.18 | / |

Note:/:No test.
Table 3 report the pharmacokinetics parameters as the mean of 3 independent experiments.

solid; $^1$H NMR (400 MHz, DMSO-$d_6$) $\delta$ 12.31 (s, 1H), 6.38 (d, $J$ = 9.3 Hz, 1H), 4.52 (s, 1H), 4.24–4.16 (m, 1H), 3.77 (s, 1H), 2.61 (s, 1H), 1.88–1.82 (m, 1H), 1.66 (q, $J$ = 14.0, 10.3 Hz, 3H), 1.41 (s, 2H), 1.37 (s, 9H), 0.95 (s, 9H). $^{13}$C NMR (101 MHz, DMSO-$d_6$) $\delta$ 171.65, 168.77, 155.88, 78.56, 63.97, 58.76, 58.54, 41.12, 35.49, 35.17, 31.31, 28.62, 27.73, 26.69.

ESI-MS $m/z$ 355.04 $[M + H]^+$.

#### *4.2.7. Synthesis of tert-butyl((S)-1-((1R,3S,4S)-3-(((S)-1-amino-1-oxo-3-((S)-2-oxopyrrolidin-3-yl) propan-2-yl)carbamoyl)-2-azabicyclo[2.2.1] heptan-2-yl)-3,3-dimethyl-1-oxobutan-2-yl)carbamate (**1-5b**)*

Compound **1-5b** was synthesized from compound **1**–**4** with compound **1-3b** using methods similar to the method described for the preparation of **1-5a**. Yield 66.7%; white solid; $^1$H NMR (400 MHz, DMSO-$d_6$) $\delta$ 8.03 (d, $J$ = 8.7 Hz, 1H), 7.54 (s, 1H), 7.26 (s, 1H), 7.01 (s, 1H), 6.48 (d, $J$ = 9.3 Hz, 1H), 4.46 (s, 1H), 4.22 (dd, $J$ = 29.0, 9.7 Hz, 2H), 3.86 (s, 1H), 3.08 (dt, $J$ = 24.7, 8.9 Hz, 2H), 2.54 (s, 1H), 2.37 (q, $J$ = 15.0, 8.8 Hz, 2H), 2.18–2.14 (m, 1H), 2.08 (d, $J$ = 37.0 Hz, 1H), 1.94 (d, $J$ = 8.6 Hz, 1H), 1.89 (s, 1H), 1.64 (s, 3H), 1.59 (d, $J$ = 11.3 Hz, 1H), 1.55–1.44 (m, 1H), 1.37 (s, 9H), 0.94 (s, 9H). $^{13}$C NMR (101 MHz, DMSO-$d_6$) $\delta$ 179.22, 174.10, 172.46, 170.14, 155.99, 78.47, 64.95, 58.62, 50.88, 41.48, 37.92, 35.47, 35.07, 34.59, 31.33, 28.63, 28.04, 27.83, 26.78, 21.50. ESI-MS $m/z$ 508.56 $[M + H]^+$.

#### *4.2.8. Synthesis of (1R,3S,4S)-N-((S)-1-cyano-2-((S)-2-oxopyrrolidin-3-yl)ethyl)-2-((S)-3,3-dimethyl-2-(2,2,2-trifluoroacetamido)butanoyl)-2-azabicyclo[2.2.1]heptane-3-carboxamide (**1b**)*

The synthesis of **1b** was achieved from **1 to 5b** using a procedure similar to that described for the preparation of **1a**. Yield 23.0%; white solid; $^1$H NMR (400 MHz, DMSO-$d_6$) $\delta$ 9.27 (d, $J$ = 8.7 Hz, 1H), 8.85 (d, $J$ = 8.6 Hz, 1H), 7.65 (s, 1H), 4.96 (ddd, $J$ = 10.8, 8.6, 5.2 Hz, 1H), 4.67–4.52 (m, 2H), 3.77 (s, 1H), 3.21–2.98 (m, 2H), 2.39 (qd, $J$ = 10.0, 4.3 Hz, 1H), 2.18–2.11 (m, 1H), 2.08 (d, $J$ = 5.3 Hz, 3H), 1.76–1.62 (m, 4H), 1.62–1.53 (m, 1H), 1.36 (dd, $J$ = 21.9, 10.1 Hz, 2H), 1.00 (s, 9H). $^{13}$C NMR (101 MHz, DMSO-$d_6$) $\delta$ 178.09, 169.93, 166.33, 157.28, 117.79, 114.93, 64.62, 58.67, 58.13, 41.60, 38.17, 37.24, 35.43, 35.36, 34.80, 31.15, 31.09, 27.90, 27.40, 26.61. ESI-HRMS Calcd for $C_{22}H_{29}F_3N_5O_4$.

$[M-H]^-$: 484.2177, found 484.2175. HPLC: t = 7.864 min, 96.1% purity.

#### *4.2.9. Synthesis of methyl(S)-5-((S)-2-((tert-butoxycarbonyl)amino)-3,3-dimethylbutanoyl)-5-azaspiro[2.4]heptane-6-carboxylate (**1-2c**)*

Compound **1-2c** was synthesized from compound **1-1c** with *N*-Boc-L-*tert*-leucine using methods similar to the method described for the preparation of **1-2a**. Yield 82.9%; colourless oil; $^1$H NMR (400 MHz, DMSO-$d_6$) $\delta$ 6.59 (d, $J$ = 9.1 Hz, 1H), 4.48 (dd, $J$ = 8.6, 5.4 Hz, 1H), 4.14–4.01 (m, 1H), 3.62 (s, 3H), 3.54 (d, $J$ = 9.8 Hz, 1H), 3.36 (s, 1H), 2.17 (dd, $J$ = 12.7, 8.6 Hz, 1H), 1.79 (dd, $J$ = 12.7, 5.5 Hz, 1H), 1.37 (s, 9H), 0.95 (s, 9H), 0.57 (ttd, $J$ = 11.7, 7.6, 6.7, 3.1 Hz, 4H). $^{13}$C NMR (101 MHz, DMSO-$d_6$) $\delta$ 172.36, 170.30, 156.04, 78.65, 59.05, 55.29, 52.13, 37.00, 35.13, 28.63, 26.66, 21.72, 10.78, 9.75. ESI-MS $m/z$ 369.28 $[M + H]^+$.

#### *4.2.10. Synthesis of (S)-5-((S)-2-((tert-butoxycarbonyl)amino)-3,3-dimethylbutanoyl)-5-azaspiro [2.4]heptane-6-carboxylic acid (**1-3c**)*

The compound **1-3c** was synthesized from **1 to 2c** using a procedure similar to that described for the preparation of **1-3a**. Yield 96.0%; white solid; $^1$H NMR (400 MHz, DMSO-$d_6$) $\delta$ 12.31 (s, 1H), 6.56 (d, $J$ = 9.1 Hz, 1H), 4.39 (dd, $J$ = 8.6, 5.4 Hz, 1H), 4.07 (t, $J$ = 4.9 Hz, 1H), 3.63 (d, $J$ = 9.8 Hz, 1H), 3.53 (d, $J$ = 9.8 Hz, 1H), 2.14 (dd, $J$ = 12.6, 8.6 Hz, 1H), 1.80 (dd, $J$ = 12.7, 5.4 Hz, 1H), 1.37 (s, 9H), 0.95 (s, 9H), 0.66–0.46 (m, 4H). $^{13}$C NMR (101 MHz, DMSO-$d_6$) $\delta$ 173.34, 170.17, 156.03, 78.61, 58.90, 55.36, 37.13, 35.20, 28.63, 26.71, 21.62, 10.87, 9.91. ESI-MS $m/z$ 355.04 $[M + H]^+$.

#### *4.2.11. Synthesis of tert-butyl((S)-1-((S)-6-(((S)-1-amino-1-oxo-3-((S)-2-oxopyrrolidin-3-yl)propan-2-yl)carbamoyl)-5-azaspiro[2.4]heptan-5-yl)-3,3-dimethyl-1-oxobutan-2-yl)carbamate (**1-5c**)*

Compound **1-5c** was synthesized from compound **1**–**4** with compound **1-3c** using methods similar to the method described for the preparation of **1-5a**. Yield 55.9%; white solid; $^1$H NMR (400 MHz, DMSO-$d_6$) $\delta$ 8.07 (d, $J$ = 8.6 Hz, 1H), 7.56 (s, 1H), 7.24 (s, 1H), 7.01 (s, 1H), 6.64 (d, $J$ = 9.1 Hz, 1H), 4.45 (t, $J$ = 7.5 Hz, 1H), 4.26 (ddd, $J$ = 12.2, 8.6, 3.6 Hz, 1H), 4.05 (d, $J$ = 8.9 Hz, 1H), 3.61 (d, $J$ = 9.8 Hz, 1H), 3.54 (d, $J$ = 9.8 Hz, 1H), 3.13 (t, $J$ = 9.2 Hz, 1H), 3.05 (td, $J$ = 9.2, 6.9 Hz, 1H), 2.48–2.39 (m, 1H), 2.19 (dt, $J$ = 13.8, 7.7 Hz, 1H), 1.91 (dtd, $J$ = 19.3, 13.0, 12.4, 5.5 Hz, 3H), 1.63 (dq, $J$ = 11.8, 9.2 Hz, 1H), 1.49 (ddd, $J$ = 14.1, 10.9, 3.4 Hz, 1H), 1.37 (s, 9H), 0.93 (s, 9H), 0.63 (dt, $J$ = 11.7, 4.3 Hz, 1H), 0.59–0.46 (m, 3H). $^{13}$C NMR (101 MHz, DMSO-$d_6$) $\delta$ 179.24, 174.04, 171.68, 170.19, 156.13, 78.56, 60.61, 58.83, 55.82, 50.97, 37.91, 37.62, 35.14, 34.61, 28.63, 26.78, 21.88, 11.59, 9.26. ESI-MS $m/z$ 508.56 $[M + H]^+$.

#### *4.2.12. Synthesis of (S)-N-((S)-1-cyano-2-((S)-2-oxopyrrolidin-3-yl) ethyl)-5-((S)-3,3-dimethyl-2-(2,2,2-trifluoroacetamido)butanoyl)-5-azaspiro[2.4]heptane-6-carboxamide (**1c**)*

The synthesis of **1c** was achieved from **1 to 5c** using a procedure similar to that described for the preparation of **1a**. Yield 49.6%; white solid; $^1$H NMR (400 MHz, DMSO-$d_6$) $\delta$ 9.38 (d, $J$ = 8.6 Hz, 1H), 8.87 (d, $J$ = 8.6 Hz, 1H), 7.66 (s, 1H), 4.98 (ddd, $J$ = 10.9, 8.5, 5.1 Hz, 1H), 4.48 (d, $J$ = 8.7 Hz, 1H), 4.38 (t, $J$ = 7.5 Hz, 1H), 3.68 (d, $J$ = 9.8 Hz, 1H), 3.51 (d, $J$ = 9.8 Hz, 1H), 3.20–3.11 (m, 1H), 3.06 (td, $J$ = 9.3, 7.0 Hz, 1H), 2.44 (qd, $J$ = 8.2, 6.2, 3.0 Hz, 1H), 2.21–2.10 (m, 2H), 2.00 (dd, $J$ = 12.6, 8.1 Hz, 1H), 1.86 (dd, $J$ = 12.6, 7.0 Hz, 1H), 1.77–1.65 (m, 2H), 0.99 (s, 9H), 0.73–0.48 (m, 4H). $^{13}$C NMR (101 MHz, DMSO-$d_6$) $\delta$ 178.12, 171.58, 167.98, 157.06, 117.77, 114.91, 60.41, 58.36, 55.92, 38.22, 37.60, 37.22, 35.54, 34.81, 27.42, 26.64, 21.92, 11.63, 9.22. ESI-HRMS Calcd for $C_{22}H_{29}F_3N_5O_4$ $[M-H]^-$: 484.2177, found 484.2175. HPLC: t = 8.150 min, 99.8% purity.

#### *4.2.13. Synthesis of methyl N-((R)-2-((tert-butoxycarbonyl)amino)-3,3-dimethylbutanoyl)-N-methyl-L-leucinate (**1-2d**)*

Compound **1-2d** was synthesized from compound **1-1d** with *N*-Boc-L-*tert*-leucine using methods similar to the method described for the preparation of **1-2a**. Yield 66.1%; white solid; $^1$H NMR (400 MHz, DMSO-$d_6$) $\delta$ 6.60 (d, $J$ = 9.1 Hz, 1H), 5.25 (dd, $J$ = 11.6, 4.2 Hz, 1H), 4.35 (t, $J$ = 4.6 Hz, 1H), 3.61 (s, 3H), 2.98 (s, 3H), 1.75 (ddd, $J$ = 14.9, 11.6, 3.7 Hz, 1H), 1.56 (ddd, $J$ = 14.1, 10.1, 4.2 Hz, 1H), 1.47–1.38 (m, 1H), 1.36 (s, 9H), 0.96 (s, 9H), 0.86 (d, $J$ = 6.6 Hz, 3H), 0.80 (d, $J$ = 6.4 Hz, 3H). $^{13}$C NMR (101 MHz, DMSO-$d_6$) $\delta$ 172.89, 172.19, 156.32, 78.64, 56.70, 54.14, 52.38, 36.94, 34.50, 32.24, 28.53, 26.81, 24.34, 21.66. ESI-MS $m/z$ 373.07 $[M + H]^+$.

#### *4.2.14. Synthesis of N-((R)-2-((tert-butoxycarbonyl)amino)-3,3-dimethylbutanoyl)-N-methyl-L-leucine (**1-3d**)*

The compound **1-3d** was synthesized from **1 to 2d** using a procedure similar to that described for the preparation of **1-3a**. Yield 98.5%; white solid; $^1$H NMR (400 MHz, DMSO-$d_6$) $\delta$ 12.67 (s, 1H), 6.55 (d, $J$ = 9.2 Hz, 1H), 5.20 (dd, $J$ = 11.7, 4.1 Hz, 1H), 4.41–4.31 (m, 1H), 2.97 (s, 3H), 1.71 (td, $J$ = 13.0, 11.7, 3.8 Hz, 1H), 1.62–1.48 (m, 2H), 1.36 (s, 9H), 0.96 (s, 9H), 0.82 (dd, $J$ = 23.4, 6.5 Hz, 6H). $^{13}$C NMR (101 MHz, DMSO-$d_6$) $\delta$ 173.42, 172.77, 156.27, 78.61, 56.66, 53.81, 37.07, 34.55, 31.97, 28.52, 26.86, 24.43, 21.69. ESI-MS $m/z$ 359.04 $[M + H]^+$.

#### *4.2.15. Synthesis of tert-butyl((R)-1-(((S)-1-(((S)-1-amino-1-oxo-3-((S)-2-oxopyrrolidin-3-yl)propan-2-yl)amino)-4-methyl-1-oxopentan-2-yl) (methyl)amino)-3,3-dimethyl-1-oxobutan-2-yl)carbamate (**1-5d**)*

Compound **1-5d** was synthesized from compound **1**–**4** with compound **1-3d** using methods similar to the method described for the preparation of **1-5a**. Yield 41.2%; white solid; $^1$H NMR (400 MHz, DMSO-$d_6$) $\delta$ 7.89 (d, $J$ = 8.2 Hz, 1H), 7.60 (s, 1H), 7.28 (s, 1H), 7.01 (s,

1H), 6.53 (d, $J = 9.2$ Hz, 1H), 5.16 (dd, $J = 10.7$, 5.0 Hz, 1H), 4.34 (d, $J = 9.2$ Hz, 1H), 4.19 (ddd, $J = 11.8$, 8.2, 4.1 Hz, 1H), 3.15 (t, $J = 9.2$ Hz, 1H), 3.09–3.04 (m, 1H), 3.01 (s, 3H), 2.21–2.13 (m, 1H), 2.13–2.03 (m, 1H), 2.01–1.92 (m, 1H), 1.67 (d, $J = 3.6$ Hz, 1H), 1.66–1.63 (m, 1H), 1.61 (dd, $J = 7.7$, 3.5 Hz, 1H), 1.54–1.48 (m, 1H), 1.48–1.43 (m, 1H), 1.36 (s, 9H), 0.93 (s, 9H), 0.86 (d, $J = 6.4$ Hz, 3H), 0.81 (d, $J = 6.3$ Hz, 3H). $^{13}$C NMR (101 MHz, DMSO-$d_6$) $\delta$ 178.66, 173.89, 172.45, 171.28, 156.25, 78.63, 56.83, 53.92, 51.35, 38.17, 37.30, 34.64, 34.05, 31.73, 27.79, 26.86, 24.57, 23.78, 22.03. ESI-MS $m/z$ 512.54 $[M + H]^+$.

#### 4.2.16. Synthesis of (S)-N-((S)-1-cyano-2-((S)-2-oxopyrrolidin-3-yl) ethyl)-4-methyl-2-((R)-N,3,3-trimethyl-2-(2,2,2-trifluoroacetamido) butanamido)pentanamide (1d)

The synthesis of **1d** was achieved from **1 to 5d** using a procedure similar to that described for the preparation of **1a**. Yield 42.7%; white solid; $^1$H NMR (400 MHz, DMSO-$d_6$) $\delta$ 9.30 (d, $J = 8.7$ Hz, 1H), 8.86 (d, $J = 7.9$ Hz, 1H), 7.72 (s, 1H), 4.99 (dd, $J = 9.9$, 5.8 Hz, 1H), 4.92 (ddd, $J = 9.6$, 7.9, 6.5 Hz, 1H), 4.81 (d, $J = 8.8$ Hz, 1H), 3.20–3.07 (m, 2H), 3.05 (s, 3H), 2.25 (qd, $J = 9.3$, 5.4 Hz, 1H), 2.16–2.05 (m, 2H), 1.81–1.74 (m, 1H), 1.73–1.67 (m, 1H), 1.63 (dt, $J = 10.0$, 4.7 Hz, 1H), 1.60–1.52 (m, 1H), 1.42–1.31 (m, 1H), 0.97 (s, 9H), 0.89 (d, $J = 6.6$ Hz, 3H), 0.82 (d, $J = 6.5$ Hz, 3H). $^{13}$C NMR (101 MHz, DMSO-$d_6$) $\delta$ 177.87, 171.21, 170.34, 157.35, 117.78, 114.92, 56.21, 54.73, 38.73, 37.54, 37.35, 35.50, 33.84, 32.62, 27.42, 26.69, 25.03, 23.39, 21.88. ESI-HRMS Calcd for $C_{22}H_{33}F_3N_5O_4$ $[M-H]^-$: 488.2490, found 488.2487. HPLC: t = 16.566 min, 96.0% purity.

#### 4.2.17. Synthesis of methyl(S)-4-((S)-2-((tert-butoxycarbonyl)amino)-3,3-dimethylbutanoyl) morpholine-3-carboxylate (1-2e)

Compound **1-2e** was synthesized from compound **1-1e** with *N*-Boc-L-*tert*-leucine using methods similar to the method described for the preparation of **1-2a**. Yield 59.5%; white solid; $^1$H NMR (400 MHz, DMSO-$d_6$) $\delta$ 5.07 (d, $J = 3.4$ Hz, 1H), 4.45 (dt, $J = 13.6$, 4.9 Hz, 1H), 4.24 (d, $J = 3.3$ Hz, 1H), 4.20 (d, $J = 12.2$ Hz, 1H), 4.08–3.96 (m, 1H), 3.83 (dd, $J = 10.7$, 7.6 Hz, 2H), 3.69 (s, 3H), 3.64 (s, 1H), 3.54 (dt, $J = 16.2$, 8.6, 7.2, 3.9 Hz, 1H), 1.39 (d, $J = 5.0$ Hz, 9H), 0.94 (d, $J = 7.0$ Hz, 9H). $^{13}$C NMR (101 MHz, DMSO-$d_6$) $\delta$ 171.68, 170.39, 156.00, 78.53, 67.73, 66.49, 55.84, 52.76, 52.24, 44.43, 35.51, 28.60, 26.75. ESI-MS $m/z$ 359.05 $[M + H]^+$.

#### 4.2.18. Synthesis of (S)-4-((S)-2-((tert-butoxycarbonyl)amino)-3,3-dimethylbutanoyl)morpholine-3-carboxylic acid (1-3e)

The compound **1-3e** was synthesized from **1 to 2e** using a procedure similar to that described for the preparation of **1-3a**. Yield 97.7%; white solid; $^1$H NMR (400 MHz, DMSO-$d_6$) $\delta$ 12.90 (s, 1H), 6.64 (d, $J = 9.2$ Hz, 1H), 4.94 (d, $J = 3.7$ Hz, 1H), 4.50–4.39 (m, 1H), 4.37–4.19 (m, 1H), 3.99 (d, $J = 12.2$ Hz, 1H), 3.88–3.78 (m, 1H), 3.50 (ddd, $J = 15.8$, 8.2, 3.2 Hz, 1H), 3.42–3.26 (m, 2H), 1.37 (d, $J = 10.2$ Hz, 9H), 0.92 (d, $J = 13.9$ Hz, 9H). $^{13}$C NMR (101 MHz, DMSO-$d_6$) $\delta$ 172.45, 171.45, 155.97, 78.72, 67.95, 66.54, 56.93, 52.17, 44.45, 35.56, 28.61, 26.79. ESI-MS $m/z$ 706.05 $[2\ M + NH_4]^+$.

#### 4.2.19. Synthesis of tert-butyl((S)-1-((S)-3-(((S)-1-amino-1-oxo-3-((S)-2-oxopyrrolidin-3-yl)propan-2-yl) carbamoyl)morpholino)-3,3-dimethyl-1-oxobutan-2-yl)carbamate (1-5e)

Compound **1-5e** was synthesized from compound **1**–**4** with compound **1-3e** using methods similar to the method described for the preparation of **1-5a**. Yield 33.4%; white solid; $^1$H NMR (400 MHz, DMSO-$d_6$) $\delta$ 7.86 (d, $J = 8.6$ Hz, 1H), 7.62 (d, $J = 11.9$ Hz, 1H), 7.36 (d, $J = 6.4$ Hz, 1H), 7.08 (d, $J = 6.8$ Hz, 1H), 6.49 (d, $J = 8.2$ Hz, 1H), 4.77 (d, $J = 3.4$ Hz, 1H), 4.41 (d, $J = 8.2$ Hz, 1H), 4.38–4.30 (m, 1H), 4.27 (d, $J = 11.5$ Hz, 1H), 3.94 (d, $J = 13.3$ Hz, 1H), 3.80 (dd, $J = 11.1$, 3.4 Hz, 1H), 3.60 (ddt, $J = 15.1$, 12.2, 7.8 Hz, 1H), 3.47 (dt, $J = 12.1$, 3.1 Hz, 1H), 3.31 (s, 1H), 3.14 (dddd, $J = 17.7$, 14.8, 8.9, 3.6 Hz, 2H), 2.24–2.09 (m, 2H), 1.97 (tdd, $J = 10.4$, 7.7, 3.4 Hz, 1H), 1.67 (dddd, $J = 12.9$, 8.8, 6.1, 3.4 Hz, 1H), 1.55 (ddp, $J = 15.6$, 10.5, 5.8 Hz, 1H), 1.39 (d, $J = 5.8$ Hz, 9H), 0.90 (d, $J = 27.6$ Hz, 9H). $^{13}$C NMR (101 MHz, DMSO-$d_6$) $\delta$ 178.72, 173.68, 171.55, 169.07, 155.98, 78.82, 68.53, 66.17, 55.38, 52.91, 51.16, 44.12, 38.20, 35.14, 34.44, 28.68, 27.86, 26.84. ESI-MS $m/z$ 498.30 $[M + H]^+$.

#### 4.2.20. Synthesis of (S)-N-((S)-1-cyano-2-((S)-2-oxopyrrolidin-3-yl) ethyl)-4-((S)-3,3-dimethyl-2-(2,2,2-trifluoroacetamido)butanoyl) morpholine-3-carboxamide (1e)

The synthesis of **1e** was achieved from **1 to 5e** using a procedure similar to that described for the preparation of **1a**. Yield 43.5%; white solid; $^1$H NMR (400 MHz, DMSO-$d_6$) $\delta$ 9.35 (d, $J = 8.4$ Hz, 1H), 8.59 (d, $J = 8.0$ Hz, 1H), 7.72 (d, $J = 5.2$ Hz, 1H), 5.06–4.96 (m, 1H), 4.89 (d, $J = 8.4$ Hz, 1H), 4.72 (d, $J = 3.7$ Hz, 1H), 4.24 (dd, $J = 12.2$, 4.9 Hz, 1H), 4.05–3.94 (m, 1H), 3.84 (dt, $J = 12.1$, 5.9 Hz, 1H), 3.63–3.54 (m, 1H), 3.50–3.43 (m, 1H), 3.43–3.38 (m, 1H), 3.29–3.07 (m, 2H), 2.35–2.22 (m, 1H), 2.15 (dddt, $J = 11.3$, 9.2, 5.3, 2.6 Hz, 1H), 2.11–1.96 (m, 1H), 1.81 (dt, $J = 13.5$, 8.3 Hz, 1H), 1.76–1.63 (m, 1H), 0.97 (d, $J = 20.4$ Hz, 9H). $^{13}$C NMR (101 MHz, DMSO-$d_6$) $\delta$ 177.85, 170.09, 169.07, 157.05, 117.77, 114.91, 68.06, 66.02, 55.70, 53.16, 44.26, 39.06, 37.61, 35.52, 35.05, 34.07, 27.51, 26.72. ESI-HRMS Calcd for $C_{20}H_{27}F_3N_5O_5$ $[M-H]^-$: 474.1970, found 474.1965. HPLC: t = 10.992 min, 99.2% purity.

#### 4.2.21. Synthesis of methyl (1R,2S)-1-((S)-2-((tert-butoxycarbonyl) amino)-3,3-dimethylbutanamido)-2-vinylcyclopropane-1-carboxylate (1-2f)

Compound **1-2f** was synthesized from compound **1-1f** with *N*-Boc-L-*tert*-leucine using methods similar to the method described for the preparation of **1-2a**. Yield 71.7%; colourless oil; $^1$H NMR (400 MHz, DMSO-$d_6$) $\delta$ 8.69 (s, 1H), 5.69–5.54 (m, 1H), 5.27 (dd, $J = 17.2$, 2.0 Hz, 1H), 5.09 (dd, $J = 10.2$, 2.0 Hz, 1H), 3.78 (t, $J = 4.9$ Hz, 1H), 3.57 (s, 3H), 2.10 (q, $J = 8.7$ Hz, 1H), 1.65 (dd, $J = 7.9$, 5.2 Hz, 1H), 1.39 (s, 9H), 1.28–1.22 (m, 1H), 0.89 (s, 9H). $^{13}$C NMR (101 MHz, DMSO-$d_6$) $\delta$ 171.64, 170.76, 155.70, 134.56, 118.11, 78.59, 62.18, 52.32, 34.66, 32.96, 28.59, 26.99, 22.89, 21.50. ESI-MS $m/z$ 355.30 $[M + H]^+$.

#### 4.2.22. Synthesis of (1R,2S)-1-((S)-2-((tert-butoxycarbonylamino)-3,3-dimethylbutanamido)-2-vinylcyclopropane-1-carboxylic acid (1-3f)

The compound **1-3f** was synthesized from **1 to 2f** using a procedure similar to that described for the preparation of **1-3a**. Yield 99.5%; white solid; $^1$H NMR (400 MHz, DMSO-$d_6$) $\delta$ 12.34 (s, 1H), 8.60 (s, 1H), 6.27 (d, $J = 9.6$ Hz, 1H), 5.76–5.60 (m, 1H), 5.26 (dd, $J = 17.2$, 2.0 Hz, 1H), 5.07 (dd, $J = 10.3$, 2.1 Hz, 1H), 3.86–3.72 (m, 1H), 2.04 (q, $J = 8.8$ Hz, 1H), 1.60 (dd, $J = 7.8$, 5.1 Hz, 1H), 1.38 (s, 9H), 1.27–1.15 (m, 1H), 0.88 (s, 9H). $^{13}$C NMR (101 MHz, DMSO-$d_6$) $\delta$ 171.94, 171.33, 155.65, 135.19, 117.51, 78.59, 62.09, 34.87, 32.85, 28.60, 27.01, 22.72, 21.49. ESI-MS $m/z$ 698.67 $[2\ M + NH_4]^+$.

#### 4.2.23. Synthesis of tert-butyl((S)-1-(((1R,2S)-1-(((S)-1-amino-1-oxo-3-((S)-2-oxopyrrolidin-3-yl) propan-2-yl)carbamoyl)-2-vinylcyclopropyl) amino)-3,3-dimethyl-1-oxobutan-2-yl)carbamate (1-5f)

Compound **1-5f** was synthesized from compound **1**–**4** with compound **1-3f** using methods similar to the method described for the preparation of **1-5a**. Yield 44.5%; white solid; $^1$H NMR (400 MHz, DMSO-$d_6$) $\delta$ 8.67 (s, 1H), 7.55 (s, 1H), 7.44 (d, $J = 8.5$ Hz, 1H), 7.16 (d, $J = 15.0$ Hz, 2H), 6.69 (d, $J = 7.1$ Hz, 1H), 5.60 (dt, $J = 17.3$, 9.7 Hz, 1H), 5.20 (dd, $J = 17.2$, 2.0 Hz, 1H), 4.99 (dd, $J = 10.1$, 2.1 Hz, 1H), 4.34–4.24 (m, 1H), 3.63 (d, $J = 7.2$ Hz, 1H), 3.13 (t, $J = 9.1$ Hz, 1H), 3.09–2.99 (m, 1H), 2.17–2.10 (m, 2H), 2.10–1.98 (m, 1H), 1.92 (s, 1H), 1.71–1.65 (m, 1H), 1.64–1.50 (m, 1H), 1.39 (s, 9H), 1.28 (d, $J = 41.6$ Hz, 1H), 1.07 (dd, $J = 9.3$, 5.0 Hz, 1H), 0.92 (s, 9H). $^{13}$C NMR (101 MHz, DMSO-$d_6$) $\delta$ 178.67, 173.58, 173.01, 172.45, 156.44, 135.42, 116.85, 78.96, 63.63, 51.43, 41.51, 38.01, 33.88, 32.13, 28.72, 28.07, 27.20, 21.50, 21.21. ESI-MS $m/z$ 494.50 $[M + H]^+$.

#### 4.2.24. Synthesis of (1R,2S)-N-((S)-1-cyano-2-((S)-2-oxopyrrolidin-3-yl) ethyl)-1-((S)-3,3-dimethyl-2-(2,2,2-trifluoroacetamido)butanamido)-2-vinylcyclopropane-1-carboxamide (1f)

The synthesis of **1f** was achieved from **1 to 5f** using a procedure similar to that described for the preparation of **1a**. Yield 41.2%; white solid; $^1$H NMR (400 MHz, DMSO-$d_6$) $\delta$ 9.21 (d, $J$ = 7.9 Hz, 1H), 8.89 (s, 1H), 8.16 (d, $J$ = 8.4 Hz, 1H), 7.65 (s, 1H), 5.59 (ddd, $J$ = 17.1, 10.3, 8.8 Hz, 1H), 5.21 (dd, $J$ = 17.2, 2.0 Hz, 1H), 5.04 (dd, $J$ = 10.3, 2.0 Hz, 1H), 4.98 (ddd, $J$ = 9.9, 5.9, 4.2 Hz, 1H), 4.18–4.11 (m, 1H), 3.14 (t, $J$ = 9.3 Hz, 1H), 3.06 (td, $J$ = 9.2, 7.1 Hz, 1H), 2.28 (qd, $J$ = 9.7, 6.2 Hz, 1H), 2.13 (t, $J$ = 5.0 Hz, 1H), 2.11–2.09 (m, 1H), 2.09–2.06 (m, 1H), 2.04 (d, $J$ = 8.8 Hz, 1H), 1.77–1.72 (m, 1H), 1.71–1.67 (m, 1H), 1.67–1.60 (m, 1H), 0.96 (s, 9H). $^{13}$C NMR (101 MHz, DMSO-$d_6$) $\delta$ 177.92, 170.36, 169.10, 157.64, 134.75, 119.88, 117.47, 114.87, 61.85, 41.25, 38.85, 37.28, 34.73, 33.85, 32.06, 29.48, 27.44, 27.02, 21.22. ESI-HRMS Calcd for $C_{21}H_{27}F_3N_5O_4$ [M−H]$^-$: 470.2021, found 470.2017. HPLC: t = 6.600 min, 96.3% purity.

### 4.3. General synthetic procedure for the preparation 2(a–d)

#### 4.3.1. Synthesis of methyl(1R,2S,5S)-3-((S)-2-((tert-butoxycarbonyl) amino)-3,3-dimethylbutanoyl)-6,6-dimethyl-3-azabicyclo[3.1.0]hexane-2-carboxylate (2–2)

Compound **2–1** (5.5 g, 26.7 mmol) and (S)-2-((*tert*-butoxycarbonyl) amino)-3,3-dimethylbutanoic acid (5.6 g, 24.2 mmol) were dissolved in DCM/DMF (V:V = 1:1, 60 mL) solution. Then 4-Methylmorpholine (7.3 g, 72.3 mmol), BOP (11.8 g, 26.7 mmol) were added to the reaction at 25 °C and stirred for 10 h. Then DCM (60 mL) and 1 N HCl aqueous solution (10 mL) were added to the reaction. After separation, the organic phase was washed with $H_2O$ (40 mL), the organic phase was washed with saturated brine (20 mL), dried over anhydrous sodium sulphate, evaporated in vacuum and purified by column chromatography (silica gel, PE/EA = 20/1 ~ 8/1) to give the compound **2–2**. Yield 63.0%; colourless oil; $^1$H NMR (400 MHz, DMSO-$d_6$) $\delta$ 6.71 (d, $J$ = 9.3 Hz, 1H), 4.21 (s, 1H), 4.09–4.03 (m, 1H), 3.93 (d, $J$ = 10.4 Hz, 1H), 3.83–3.76 (m, 1H), 3.65 (s, 3H), 1.52 (dt, $J$ = 8.6, 4.4 Hz, 1H), 1.41 (d, $J$ = 7.6 Hz, 1H), 1.35 (s, 9H), 1.01 (s, 3H), 0.94 (s, 9H), 0.85 (s, 3H). $^{13}$C NMR (101 MHz, DMSO-$d_6$) $\delta$ 171.99, 170.67, 156.38, 78.70, 59.22, 52.37, 47.51, 34.49, 30.04, 28.52, 26.72, 19.42, 12.59. ESI-MS $m/z$ 383.30 [M + H]$^+$.

#### 4.3.2. Synthesis of (1R,2S,5S)-3-((S)-2-((tert-butoxycarbonyl)amino)-3,3-dimethylbutanoyl)-6,6-dimethyl-3-azabicyclo[3.1.0]hexane-2-carboxylic acid (2–3)

Compound **2–2** (5.7 g, 14.9 mmol), lithium hydroxide (2.4 g, 59.2 mmol) and water (65 mL) were dissolved in THF (65 mL) solution at 40 °C and stirred for 2 h. Then 1 N HCl aqueous solution was added to the reaction to adjust the pH 2–3. EA (100 mL) was added to the solution and separation, the organic phase was washed with saturated brine (30 mL), dried over anhydrous sodium sulphate, evaporated in vacuum and purified by column chromatography (silica gel, DCM/MeOH = 100/1–30/1) to give the compound **2–3**. Yield 90.9%; white solid; $^1$H NMR (400 MHz, DMSO-$d_6$) $\delta$ 12.44 (s, 1H), 6.66 (d, $J$ = 9.5 Hz, 1H), 4.13 (s, 1H), 4.08–4.03 (m, 1H), 3.91 (d, $J$ = 10.4 Hz, 1H), 3.78 (tq, $J$ = 8.8, 4.3, 3.8 Hz, 1H), 1.50 (dd, $J$ = 7.6, 5.0 Hz, 1H), 1.39 (d, $J$ = 7.6 Hz, 1H), 1.35 (s, 9H), 1.01 (s, 3H), 0.93 (s, 9H), 0.84 (s, 3H). $^{13}$C NMR (101 MHz, DMSO-$d_6$) $\delta$ 173.06, 170.52, 156.38, 78.67, 59.34, 59.02, 47.51, 34.56, 30.24, 28.53, 26.78, 21.49, 19.28, 12.66. ESI-MS $m/z$ 369.30 [M + H]$^+$.

#### 4.3.3. Synthesis of tert-butyl((S)-1-((1R,2S,5S)-2-(((S)-1-amino-1-oxo-3-((S)-2-oxopyrrolidin-3-yl)propan-2-yl)carbamoyl)-6,6-dimethyl-3-azabicyclo[3.1.0]hexan-3-yl)-3,3-dimethyl-1-oxobutan-2-yl)carbamate (2–4)

Compound **1–4** (3.7 g, 13.6 mmol) and 4 N HCl in 1,4-dioxane (4 mL) were dissolved in DCM (6 mL), the reaction was stirred at 25 °C for 2 h. The reaction was concentrated to remove the solvent and dry HCl salt was obtained. Meanwhile, compound **2–3** (5.0 g, 13.6 mmol) and HATU (7.7 g, 20.3 mmol) were dissolved in DCM (20 mL), the reaction was stirred at 25 °C for 30 min. Then *N, N*-Diisopropylethylamine (3.9 g, 29.9 mmol) and HCl salt were added to the reaction, the reaction was stirred at 25 °C for 10 h. Then DCM (40 mL) and 1 N HCl aqueous solution (10 mL) were added to the reaction. After separation, the organic phase was washed with $H_2O$ (10 mL), the organic phase was washed with saturated brine (10 mL), dried over anhydrous sodium sulphate, evaporated in vacuum and purified by column chromatography (silica gel, DCM/MeOH = 150/1–20/1) to give the compound **2–4**. Yield 45.1%; white solid; $^1$H NMR (400 MHz, DMSO-$d_6$) $\delta$ 8.23 (d, $J$ = 8.7 Hz, 1H), 7.54 (s, 1H), 7.27 (s, 1H), 7.02 (s, 1H), 6.61 (d, $J$ = 9.3 Hz, 1H), 4.34–4.20 (m, 2H), 4.07–3.98 (m, 1H), 3.89–3.77 (m, 2H), 3.12 (t, $J$ = 9.2 Hz, 1H), 3.02 (td, $J$ = 9.3, 7.0 Hz, 1H), 2.47–2.32 (m, 1H), 2.20–2.05 (m, 1H), 2.01–1.87 (m, 1H), 1.61 (dq, $J$ = 11.9, 9.3 Hz, 1H), 1.53–1.48 (m, 1H), 1.46 (dt, $J$ = 7.2, 3.5 Hz, 1H), 1.36 (s, 1H), 1.34 (s, 9H), 1.01 (s, 3H), 0.91 (s, 9H), 0.86 (s, 3H). $^{13}$C NMR (101 MHz, DMSO-$d_6$) $\delta$ 179.18, 174.02, 171.27, 168.88, 164.88, 136.53, 130.86, 130.53, 129.13, 124.93, 60.70, 58.51, 50.83, 48.10, 37.83, 35.33, 34.57, 31.08, 27.63, 27.08, 26.34, 19.06, 12.99. ESI-MS $m/z$ 522.34 [M + H]$^+$.

#### 4.3.4. Synthesis of (1R,2S,5S)-N-((S)-1-amino-1-oxo-3-((S)-2-oxopyrrolidin-3-yl)propan-2-yl)-3-((S)-3,3-dimethyl-2-(2,2,3,3,3-pentafluoropropanamido)butanoyl)-6,6-dimethyl-3-azabicyclo [3.1.0] hexane-2-carboxamide (2-5a)

Compound **2–4** (450 mg, 0.9 mmol) and 4 N HCl in 1,4-dioxane (3 mL) were dissolved in DCM (6 mL), the reaction was stirred at 40 °C for 1 h. The reaction was concentrated to remove the solvent. Then triethylamine (261 mg, 2.6 mmol), Perfluoropropionic anhydride (294 mg, 0.9 mmol) and DCM (6 mL) were added to the reaction at 0 °C. The reaction was allowed to warm to 25 °C, and stirred for 10 h. Then DCM (10 mL) and 1 N HCl aqueous solution (3 mL) were added to the reaction. After separation, the organic phase was washed with $H_2O$ (5 mL), the organic phase was washed with saturated brine (5 mL), dried over anhydrous sodium sulphate, evaporated in vacuum and purified by column chromatography (silica gel, DCM/MeOH = 100/1 ~ 20/1) to give the compound **2-5a**. Yield 65.4%; white solid; $^1$H NMR (400 MHz, DMSO-$d_6$) $\delta$ 9.39 (d, $J$ = 8.9 Hz, 1H), 8.29 (d, $J$ = 8.8 Hz, 1H), 7.55 (s, 1H), 7.30 (s, 1H), 7.03 (s, 1H), 4.58–4.47 (m, 1H), 4.35–4.23 (m, 2H), 3.89 (dd, $J$ = 10.3, 5.4 Hz, 1H), 3.66 (d, $J$ = 10.4 Hz, 1H), 3.13 (t, $J$ = 9.2 Hz, 1H), 3.03 (td, $J$ = 9.3, 7.0 Hz, 1H), 2.15 (tt, $J$ = 14.0, 7.7 Hz, 1H), 1.99–1.92 (m, 1H), 1.64 (dq, $J$ = 11.8, 9.2 Hz, 1H), 1.52 (d, $J$ = 13.4 Hz, 1H), 1.49 (d, $J$ = 2.6 Hz, 1H), 1.47 (s, 1H), 1.43–1.32 (m, 1H), 1.01 (s, 3H), 0.98 (s, 9H), 0.81 (s, 3H). $^{13}$C NMR (101 MHz, DMSO-$d_6$) $\delta$ 179.11, 173.98, 172.44, 171.07, 167.52, 158.21, 157.96, 60.70, 58.37, 50.82, 48.18, 37.80, 35.28, 34.55, 30.99, 27.87, 27.48, 26.70, 26.32, 21.49, 18.98, 12.66. ESI-MS $m/z$ 567.87 [M + H]$^+$.

#### 4.3.5. Synthesis of (1R,2S,5S)-N-((S)-1-cyano-2-((S)-2-oxopyrrolidin-3-yl)ethyl)-3-((S)-3,3-dimethyl-2-(2,2,3,3,3-pentafluoropropanamido) butanoyl)-6,6-dimethyl-3-azabicyclo[3.1.0]hexane-2-carboxamide (2a)

Compound **2-5a** (170 mg, 0.3 mmol) and Burgess reagent (127 mg, 0.5 mmol) were dissolved in DCM (5 mL), the reaction was stirred at 25 °C for 10 h. The reaction was purified by column chromatography (silica gel, DCM/MeOH = 150/1 ~ 40/1) to give the compound **2a**. Yield 42.5%; white solid; $^1$H NMR (400 MHz, DMSO-$d_6$) $\delta$ 9.40 (d, $J$ = 8.8 Hz, 1H), 9.02 (d, $J$ = 8.5 Hz, 1H), 7.67 (s, 1H), 4.98 (ddd, $J$ = 10.9, 8.5, 5.1 Hz, 1H), 4.51 (d, $J$ = 8.8 Hz, 1H), 4.16 (s, 1H), 3.92 (dd, $J$ = 10.4, 5.5 Hz, 1H), 3.69 (d, $J$ = 10.4 Hz, 1H), 3.22–3.12 (m, 1H), 3.05 (td, $J$ = 9.3, 7.0 Hz, 1H), 2.20–2.14 (m, 1H), 2.11 (dd, $J$ = 7.3, 4.1 Hz, 1H), 2.08 (dd, $J$ = 8.5, 5.6 Hz, 1H), 1.77–1.72 (m, 1H), 1.72–1.67 (m, 1H), 1.57 (dd, $J$ = 7.6, 5.3 Hz, 1H), 1.35–1.28 (m, 1H), 1.03 (s, 3H), 0.98 (s, 9H), 0.83 (s, 3H). $^{13}$C NMR (101 MHz, DMSO-$d_6$) $\delta$ 177.98, 171.14, 167.73, 158.30, 158.04, 157.78, 120.08, 60.51, 58.43, 48.08, 38.26, 37.21, 35.19, 34.61, 30.71, 27.70, 27.33, 26.67, 26.16, 19.23, 12.59. ESI-HRMS Calcd for $C_{24}H_{31}F_5N_5O_4$ [M−H]$^-$: 548.2302, found 548.2305.

HPLC: t = 9.669 min, 99.0% purity.

#### 4.3.6. Synthesis of (1R,2S,5S)-N-((S)-1-amino-1-oxo-3-((S)-2-oxopyrrolidin-3-yl)propan-2-yl)-3-((S)-3,3-dimethyl-2-((trifluoromethyl) sulfonamido)butanoyl)-6,6-dimethyl-3-azabicyclo[3.1.0]hexane-2-carboxamide (2-5b)

The compound **2-5b** was synthesized from **2 to 4** using a procedure similar to that described for the preparation of **2-5a**. Yield 21.0%; white solid; $^1$H NMR (400 MHz, DMSO-$d_6$) $\delta$ 9.63 (s, 1H), 8.30 (d, $J$ = 9.0 Hz, 1H), 7.51 (s, 1H), 7.32 (s, 1H), 7.01 (s, 1H), 4.31 (s, 1H), 4.31–4.25 (m, 1H), 3.87 (s, 1H), 3.48 (d, $J$ = 10.3 Hz, 1H), 3.16–3.07 (m, 1H), 3.01 (td, $J$ = 9.3, 7.1 Hz, 1H), 2.46–2.35 (m, 1H), 2.13 (dt, $J$ = 14.0, 8.0 Hz, 1H), 2.03–1.90 (m, 1H), 1.67 (dd, $J$ = 11.0, 7.8 Hz, 1H), 1.64–1.54 (m, 1H), 1.53–1.50 (m, 1H), 1.48 (s, 1H), 1.38 (d, $J$ = 7.7 Hz, 1H), 1.02 (s, 3H), 1.00 (s, 9H), 0.88 (s, 3H). $^{13}$C NMR (101 MHz, DMSO-$d_6$) $\delta$ 179.09, 173.99, 172.45, 171.06, 167.80, 63.18, 61.06, 50.66, 48.08, 37.71, 36.03, 34.73, 31.27, 28.01, 26.73, 26.33, 19.16, 12.94. ESI-MS $m/z$ 554.11 $[M + H]^+$.

#### 4.3.7. Synthesis of (1R,2S,5S)-N-((S)-1-cyano-2-((S)-2-oxopyrrolidin-3-yl)ethyl)-3-((S)-3,3-dimethyl-2-((trifluoromethyl)sulfonamido)butanoyl)-6,6-dimethyl-3-azabicyclo[3.1.0]hexane-2-carboxamide (2b)

The compound **2b** was synthesized from **2 to 5b** using a procedure similar to that described for the preparation of **2a**. Yield 57.0%; white solid; $^1$H NMR (400 MHz, DMSO-$d_6$) $\delta$ 9.65 (d, $J$ = 9.1 Hz, 1H), 9.08 (d, $J$ = 8.6 Hz, 1H), 7.65 (s, 1H), 4.97 (ddd, $J$ = 11.1, 8.6, 4.9 Hz, 1H), 4.18 (s, 1H), 3.97–3.84 (m, 2H), 3.50 (d, $J$ = 10.4 Hz, 1H), 3.14 (t, $J$ = 9.2 Hz, 1H), 3.03 (td, $J$ = 9.2, 7.0 Hz, 1H), 2.39 (td, $J$ = 10.4, 9.7, 3.9 Hz, 1H), 2.22–2.02 (m, 2H), 1.77–1.65 (m, 2H), 1.58 (dd, $J$ = 7.8, 5.5 Hz, 1H), 1.33 (d, $J$ = 7.7 Hz, 1H), 1.04 (s, 3H), 0.99 (s, 9H), 0.89 (s, 3H). $^{13}$C NMR (101 MHz, DMSO-$d_6$) $\delta$ 177.94, 171.08, 168.06, 120.09, 63.09, 60.90, 55.37, 48.02, 38.13, 37.14, 35.99, 34.78, 30.92, 28.24, 27.28, 26.66, 26.15, 19.41, 12.85. ESI-HRMS Calcd for $C_{22}H_{31}F_3N_5O_5S$ $[M-H]^-$: 534.2003, found 534.2003. HPLC: t = 12.290 min, 97.3% purity.

#### 4.3.8. Synthesis of (1R,2S,5S)-N-((S)-1-amino-1-oxo-3-((S)-2-oxopyrrolidin-3-yl)propan-2-yl)-3-((S)-2-(cyclopropanesulfonamido)-3,3-dimethylbutanoyl)-6,6-dimethyl-3-azabicyclo[3.1.0]hexane-2-carboxamide (2-5c)

The compound **2-5c** was synthesized from **2 to 4** using a procedure similar to that described for the preparation of **2-5a**. Yield 29.8%; white solid; $^1$H NMR (400 MHz, DMSO-$d_6$) $\delta$ 8.27 (d, $J$ = 8.9 Hz, 1H), 7.52 (s, 1H), 7.30 (d, $J$ = 2.1 Hz, 1H), 7.06–6.99 (m, 2H), 4.37–4.23 (m, 2H), 3.83 (dd, $J$ = 10.1, 5.5 Hz, 1H), 3.80–3.75 (m, 1H), 3.66 (d, $J$ = 10.3 Hz, 1H), 3.13 (d, $J$ = 9.4 Hz, 1H), 3.11–3.03 (m, 1H), 3.01 (dd, $J$ = 9.3, 7.2 Hz, 1H), 2.48–2.43 (m, 1H), 2.42–2.37 (m, 1H), 2.19–2.13 (m, 1H), 2.13–2.08 (m, 1H), 2.00–1.90 (m, 1H), 1.68–1.54 (m, 1H), 1.48 (qd, $J$ = 8.0, 6.7, 3.5 Hz, 2H), 1.36 (d, $J$ = 7.7 Hz, 1H), 1.01 (s, 3H), 0.97 (s, 9H), 0.90 (s, 3H), 0.89–0.84 (m, 2H). $^{13}$C NMR (101 MHz, DMSO-$d_6$) $\delta$ 179.14, 174.06, 171.31, 169.64, 61.18, 60.79, 50.73, 48.00, 37.73, 35.70, 34.59, 31.08, 27.99, 26.87, 26.44, 19.18, 13.37, 6.06, 5.07. ESI-MS $m/z$ 526.37 $[M + H]^+$.

#### 4.3.9. Synthesis of (1R,2S,5S)-N-((S)-1-cyano-2-((S)-2-oxopyrrolidin-3-yl)ethyl)-3-((S)-2-(cyclopropanesulfonamido)-3,3-dimethylbutanoyl)-6,6-dimethyl-3-azabicyclo[3.1.0]hexane-2-carboxamide (2c)

The compound **2c** was synthesized from **2 to 5c** using a procedure similar to that described for the preparation of **2a**. Yield 29.8%; white solid; $^1$H NMR (400 MHz, DMSO-$d_6$) $\delta$ 9.03 (d, $J$ = 8.6 Hz, 1H), 7.64 (s, 1H), 7.07 (d, $J$ = 9.5 Hz, 1H), 4.97 (ddd, $J$ = 11.1, 8.6, 5.0 Hz, 1H), 4.16 (s, 1H), 3.85 (dd, $J$ = 10.2, 5.6 Hz, 1H), 3.78 (d, $J$ = 9.5 Hz, 1H), 3.68 (d, $J$ = 10.3 Hz, 1H), 3.14 (d, $J$ = 9.2 Hz, 1H), 3.12–3.05 (m, 1H), 3.02 (dd, $J$ = 9.3, 7.0 Hz, 1H), 2.42 (qd, $J$ = 10.2, 4.8 Hz, 1H), 2.20–2.15 (m, 1H), 2.15–2.09 (m, 1H), 2.09–2.03 (m, 1H), 1.77–1.71 (m, 1H), 1.70 (dd, $J$ = 5.2, 2.4 Hz, 1H), 1.69–1.65 (m, 1H), 1.56 (dd, $J$ = 7.7, 5.4 Hz, 1H), 1.29 (d, $J$ = 7.7 Hz, 1H), 1.03 (s, 3H), 0.97 (s, 9H), 0.91 (s, 3H), 0.89–0.83 (m, 2H). $^{13}$C NMR (101 MHz, DMSO-$d_6$) $\delta$ 177.99, 171.35, 169.88, 120.15, 61.11, 60.59, 47.92, 38.14, 37.14, 35.64, 34.68, 31.05, 28.21, 27.30, 26.82, 26.28, 19.43, 13.29, 6.07, 5.03. ESI-HRMS Calcd for $C_{24}H_{36}N_5O_5S$ $[M-H]^-$: 506.2443, found 506.2442. HPLC: t = 7.178 min, 98.3% purity.

#### 4.3.10. Synthesis of (1R,2S,5S)-N-((S)-1-amino-1-oxo-3-((S)-2-oxopyrrolidin-3-yl)propan-2-yl)-3-((S)-2-(3,5-bis(trifluoromethyl) benzamido)-3,3-dimethylbutanoyl)-6,6-dimethyl-3-azabicyclo [3.1.0] hexane-2-carboxamide (2-5d).

The compound **2-5d** was synthesized from **2 to 4** using a procedure similar to that described for the preparation of **2-5a**. Yield 56.1%; white solid; $^1$H NMR (400 MHz, DMSO-$d_6$) $\delta$ 8.93 (d, $J$ = 8.7 Hz, 1H), 8.46 (d, $J$ = 1.7 Hz, 2H), 8.32–8.24 (m, 2H), 7.55 (s, 1H), 7.30 (d, $J$ = 2.1 Hz, 1H), 7.07–7.01 (m, 1H), 4.68 (d, $J$ = 8.7 Hz, 1H), 4.36–4.26 (m, 2H), 3.94 (dd, $J$ = 10.3, 5.4 Hz, 1H), 3.81 (d, $J$ = 10.3 Hz, 1H), 3.15 (t, $J$ = 9.1 Hz, 1H), 3.09–3.01 (m, 1H), 2.46–2.32 (m, 1H), 2.23–2.12 (m, 1H), 1.94 (ddd, $J$ = 13.5, 12.0, 3.8 Hz, 1H), 1.72–1.61 (m, 1H), 1.58–1.50 (m, 1H), 1.50–1.46 (m, 1H), 1.38 (d, $J$ = 7.7 Hz, 1H), 1.04 (s, 9H), 1.00 (s, 3H), 0.84 (s, 3H). $^{13}$C NMR (101 MHz, DMSO-$d_6$) $\delta$ 179.18, 174.02, 171.27, 168.88, 164.88, 136.53, 130.86, 130.53, 129.13, 124.93, 60.70, 58.51, 50.83, 48.10, 37.83, 35.33, 34.57, 31.08, 27.91, 27.08, 26.34, 19.06, 12.99. ESI-MS $m/z$ 662.11 $[M + H]^+$.

#### 4.3.11. Synthesis of (1R,2S,5S)-3-((S)-2-(3,5-bis(trifluoromethyl) benzamido)-3,3-dimethylbutanoyl)-N-((S)-1-cyano-2-((S)-2-oxopyrrolidin-3-yl)ethyl)-6,6-dimethyl-3-azabicyclo[3.1.0]hexane-2-carboxamide (2d)

The compound **2d** was synthesized from **2 to 5d** using a procedure similar to that described for the preparation of **2a**. Yield 40.9%; white solid; $^1$H NMR (400 MHz, DMSO-$d_6$) $\delta$ 8.99 (d, $J$ = 8.5 Hz, 1H), 8.92 (d, $J$ = 8.6 Hz, 1H), 8.45 (s, 2H), 8.29 (s, 1H), 7.66 (s, 1H), 4.98 (ddd, $J$ = 10.9, 8.5, 5.0 Hz, 1H), 4.66 (d, $J$ = 8.6 Hz, 1H), 4.16 (s, 1H), 3.96 (dd, $J$ = 10.3, 5.5 Hz, 1H), 3.83 (d, $J$ = 10.4 Hz, 1H), 3.15 (t, $J$ = 9.3 Hz, 1H), 3.05 (q, $J$ = 8.6 Hz, 1H), 2.41 (td, $J$ = 10.2, 9.6, 4.2 Hz, 1H), 2.21–2.05 (m, 2H), 1.80–1.64 (m, 2H), 1.57 (dd, $J$ = 7.7, 5.3 Hz, 1H), 1.34–1.29 (m, 1H), 1.04 (s, 9H), 1.02 (s, 3H), 0.86 (s, 3H). $^{13}$C NMR (101 MHz, DMSO-$d_6$) $\delta$ 178.01, 171.33, 169.06, 164.98, 136.51, 130.88, 130.55, 129.16, 124.93, 120.11, 60.50, 58.57, 48.01, 38.24, 38.15, 37.22, 35.24, 34.64, 30.81, 27.85, 27.04, 26.20, 19.31, 12.92. ESI-HRMS Calcd for $C_{30}H_{34}F_6N_5O_4$ $[M-H]^-$: 642.2520, found 642.2523. HPLC: t = 17.497 min, 97.4% purity.

### 4.4. Protein expression and purification

The cDNA of SARS-CoV-2 3CL$^{pro}$ (GenBank: MN908947.3) was cloned into the pGEX6p-1 vector. To obtain the SARS-CoV-2 3CL$^{pro}$ with authentic N and C terminals, four amino acids (AVLQ) were inserted between the GST tag and the full-length SARS-CoV-2 3CL$^{pro}$, while eight amino acid (GPHHHHHH) were added to the C-terminal of SARS-CoV-2 3CL$^{pro}$. The plasmid was then transformed into BL21 (DE3) cells for protein expression. The N terminal GST tag and four amino acids (AVLQ) was self-cleavable. The expressed protein with authentic N terminal was purified by a Ni-NTA column (GE Healthcare) and transformed into the cleavage buffer (150 mM NaCl, 25 mM Tris, pH 7.5) containing human rhinovirus 3C protease for removing the additional residues. The resulting protein sample was further passed through a size-exclusion chromatography (HiLoad$^{TM}$ 16/600 Superdex$^{TM}$ 200 pg, GE Healthcare). The eluted protein samples were stored in a solution (10 mM Tris, pH 7.5) for the enzymatic inhibition assay.

### 4.5. Enzymatic inhibitory activity assay

A fluorescence resonance energy transfer (FRET) protease assay was applied to measure the inhibitory activity of compounds against SARS-CoV-2 3CL$^{pro}$. The recombinant SARS-CoV-2 3CL$^{pro}$ at a concentration

of 40 nM was mixed with serial dilutions of each compound in 80 μL of assay buffer (50 mM Tris–HCl, pH 7.3, 1 mM EDTA) and incubated for 10 min. The reaction was initiated by adding 40 μL of a fluorogenic substrate (Dacyl-KTSAVLQSGFRKME-Edans) at a final concentration of 10 μM. After that, the fluorescence signal at 340 nm (excitation)/490 nm (emission) was measured immediately every every 1 min for 10 min with a Bio-Tek SynergyH1 plate reader. The velocities of reactions with compounds added at various concentrations compared to the reaction added with DMSO were calculated and used to generate inhibition profiles. For each compound, experment in triplicate was performed to determine $IC_{50}$ and SD values.

### 4.6. Anti-viral activity and cytotoxicity assays

The Vero E6 cell line was obtained from American Type Culture Collection (ATCC, Manassas, USA) and maintained in minimum Eagle's medium (MEM; Gibco Invitrogen) supplemented with 10% fetal bovine serum (FBS; Invitrogen, UK) in a humid incubator with 5% $CO_2$ at 37 °C. The cytotoxicity of tested compounds on the Vero E6 cells were determined by CCK8 assays (Beyotime, China). A clinical isolate SARS-CoV-2 was propagated in the Vero E6 cells, and the viral titer was determined by 50% tissue culture infective dose (TCID50) using immunofluorescence assay. All the infection experiments were performed at biosafety level-3 (BSL-3).

Preseeded Vero E6 cells ($5 \times 10^4$ cells/well) were incubated with different concentrations of compounds for 1 h in 48-well plate, and the virus was subsequently added (a multiplicity of infection of 0.01) to infect the cells for 2 h. After that, the virus–compound mixture was removed, and the cells were further cultured with a fresh compound-containing medium. At 24 h post infection, the cell supernatant was collected, and the viral RNA in the supernatant was submitted to quantitative real-time RT-PCR (qRT-PCR) analysis. DMSO was used in the controls. The half maximal effective concentration ($EC_{50}$) values were calculated by GraphPad Prism 8.3.0 software.

Vero E6 cells were plated in the 96-well plates at a density of $2.5 \times 10^3$ cells per well for 16 h. Then the cells were incubated with the test articles at different cocentrations (0.5–200 μM) for another 24 h (n = 3). Cell viability was determined using the CCK8 assay kit after cells were incubated. The absorbance was measured by an automatic microplate reader (Biotek, Winooski, VT, USA) at OD450. The half cytotoxicity concentration ($CC_{50}$) values for each compound were calculated by GraphPad Prism 8.3.0 software (GraphPad Software Inc., La Jolla, CA, USA).

### 4.7. Rat pharmacokinetics

Rat pharmacokinetics studies were done at Medicilon (Shanghai, China); tested male rats was administered via intravenous injection or oral administration. The blood was taken via submandibular vein or other suitable vein. Sample was placed in tubes containing K2-EDTA and stored on ice until centrifuged. The blood sample was centrifuged at 6800 g for 6 min at 2–8 °C within 1 h after collected and stored frozen at approximately −80 °C. An aliquot of 15 μL plasma sample was protein precipitated with 300 μL MeOH in which contains 100 ng/mL Warfarin (IS). The mixture was vortexed for 1 min and centrifuged at 18,000 g for 7 min. Transfer 300 μL supernatant to 96 well plates. An aliquot of 6 μL supernatant was injected for LC-MS/MS analysis. Standard set of parameters was calculated using noncompartmental analysis modules in FDA certified pharmacokinetic program Phoenix WinNonlin 7.0 (Pharsight, USA).

### 4.8. Liver microsomes metabolic stability

Human, mouse liver microsomes (from Xenotech) with final liver microsomal protein concentration of 0.5 mg/mL. 5 μL of 10 mM compound stock solution and reference solution were added to 95 μL ACN. 1.5 μL of 500 μM spiked solution and 18.75 μL of 20 mg/mL liver microsomes were added to 479.75 μL of K/Mg- buffer. NADPH stock solution (6 mM, 5 mg/mL) was prepared by dissolving NADPH into K/Mg-buffer. Dispense 30 μL of 1.5 μM spiking solution containing 0.75 mg/mL microsomes solution to the assay plates designated for different time points (0, 5, 15, 30, 45 min). Pre-incubate other plate at 37 °C for 5 min. For 0 min, added 150 μL of ACN containing IS to the wells before adding 15 μL of NADPH stock solution (6 mM). For other time points, added 15 μL of NADPH stock solution (6 mM) to the wells to start the reaction and timing. At 5 min, 15 min, 30 min, 45 min added 150 μL of ACN containing IS to the wells of corresponding plates, respectively, to stop the reaction. After quenching, shook the plates for 10 min (600 rpm) and then centrifuged at 6000 rpm for 15 min. 80 μL of the supernatant from each well was transferred to a 96-well sample plate containing 140 μL of pure water for LC/MS analysis.

## Declaration of Competing Interest

The authors declare that they have no known competing financial interests or personal relationships that could have appeared to influence the work reported in this paper.

## Data availability

Data will be made available on request.

## Acknowledgments

This research was supported by National Key Research and Development Plan of China (2021YFC2300700 to L.K.Z., 2022YFC2303300 to L.K.Z.), Shanghai Institute of Materia Medica (Grant SIMM010203) and the Strategic Priority Research Program of Chinese Academy of Sciences (SIMM****).

## Appendix A. Supplementary material

Supplementary data to this article can be found online at https://doi.org/10.1016/j.bmc.2023.117316.

## References

1 Wu F, Zhao S, Yu B, et al. Author correction: a new coronavirus associated with human respiratory disease in China. *Nature*. 2020;580:265–269. https://doi.org/10.1038/s41586-020-2202-3.
2 Zhou P, Yang XL, Wang XG, et al. Addendum: a pneumonia outbreak associated with a new coronavirus of probable bat origin. *Nature*. 2020;588:270–273. https://doi.org/10.1038/s41586-020-2012-7.
3 Levin EG, Lustig Y, Cohen C, et al. Waning immune humoral response to BNT162b2 COVID-19 vaccine over 6 months. *N Engl J Med*. 2021;385:e84.
4 Bergwerk M, Gonen T, Lustig Y, et al. COVID-19 breakthrough infections in vaccinated health care workers. *N Engl J Med*. 2021;385:1474–1484. https://doi.org/10.1056/NEJMoa2114583.
5 Hirose Y, Shindo N, Mori M, et al. Discovery of chlorofluoroacetamide-based covalent inhibitors for severe acute respiratory syndrome coronavirus 2 3CL protease. *J Med Chem*. 2022;65:13852–13865. https://doi.org/10.1021/acs.jmedchem.2c01081.
6 Berry M, Fielding BC, Gamieldien J. Potential broad spectrum inhibitors of the coronavirus 3CLpro: a virtual screening and structure-based drug design study. *Viruses*. 2015;7:6642–6660. https://doi.org/10.3390/v7122963.
7 Anand K, Ziebuhr J, Wadhwani P, Mesters JR, Hilgenfeld R. Coronavirus main proteinase (3CLpro) structure: basis for design of anti-SARS drugs. *Science*. 2003;300:1763–1767. https:// doi.org/10.1126/ science.1085658.
8 Usman B, Jennifer B, Adrian VC, Leavitt S, Freire E, Freire E. Identification of novel inhibitors of the SARS coronavirus main protease 3CLpro. *Biochemistry*. 2004;43:4906–4912. https://doi.org /10.1021/bi0361766.
9 Jin Z, Du X, Xu Y, et al. Structure of Mpro from SARS-CoV-2 and discovery of its inhibitors. *Nature*. 2020;582:289–293. https://doi.org/10.1038/s41586-020-2223-y.
10 Lu R, Zhao X, Li J, et al. novel coronavirus: implications for virus origins and receptor binding. *Lancet*. 2019;395(2020):565–574. https://doi.org/10.1016/S0140-6736(20)30251-8.
11 Kanchan A, Gottfried JP, Jeroen RM, Stuart GS, John Z, Rolf H. Structure of coronavirus main proteinase reveals combination of a chymotrypsin fold with an

extra alpha-helical domain. *EMBO J*. 2002;21:3213–3224. https://doi.org/10.1093/emboj/cdf327.
12 Xiong MY, Su HX, Zhao WF, Xie H, Shao Q, Xu YC. What coronavirus 3C-like protease tells us: from structure, substrate selectivity, to inhibitor design. *Med Res Rev*. 2021;3:1–34. https://doi.org /10.1002/med.21783.
13 Liu YZ, Liang CY, Xin L, et al. The development of Coronavirus 3C-Like protease (3CLpro) inhibitors from 2010 to 2020. *Eur J Med Chem*. 2020;206, 112711. https://www.sciencedirect.com/science/article/pii/S0223523420306838.
14 Dai W, Zhang B, Jiang XM, et al. Structure-based of antiviral drug candidates targeting the SARS-CoV-2 main protease. *Science*. 2020;368:1331–1335. https://doi.org/10.1126/science.abb4489.
15 Li J, Lin C, Zhou X, Zhong F, Zeng P, Yang Y, Zhang Y, Yu B, Fan X, McCormick PJ, Fu R, Fu Y, Jiang H, Zhang J, Rozanne SG. Structural basis of the main proteases of coronavirus bound to drug candidate PF-07321332. *J. Virol.* 2022;96:e0201321.
16 Ghosh AK, Mishevich JL, Mesecar A, Mitsuya H. Recent drug development and medicinal chemistry approaches for the treatment of SARS-CoV-2 infection and COVID-19. *Chem Med Chem*. 2022;17. https://chemistry-europe.onlinelibrary. wiley.com/doi/abs/10.1002/ cmdc.202200440 e202200440.
17 Tan B, Joyce R, Tan HZ, Hu YM, Wang J. SARS-CoV-2 main protease drug design, assay development, and drug resistance studies. *Acc Chem Res*. 2023;56:157–168. https:// pubs. acs.org/doi/full/10.1021/acs.accounts.2c00735.
18 Dai W, Jochmans D, Xie H, et al. Design, synthesis, and biological evaluation of peptidomimetic aldehydes as broad-spectrum inhibitors against enterovirus and SARS-CoV-2. *J Med Chem*. 2022;65:2794–2808. jmedchem.0c02258 https://doi.org/10.1021/acs.
19 Gao K, Wang R, Chen J, Tepe JJ, Huang F, Wei GW. Perspectives on SARS-CoV-2 main protease inhibitors. *J Med Chem*. 2021;64:16922–16955. https://doi.org/10.1021/acs. jmedchem. 1c00409.
20 Halford B. The path to Paxlovid. C&EN Global Enterprise 2022; 8: 405-407. <https:// doi.org/ 10.1021 /acscentsci.2c00369>.
21 Kneller DW, Li H, Phillips G, et al. Covalent narlaprevir-and boceprevir-derived hybrid inhibitors of SARS-CoV-2 main protease. *Nat Commun*. 2022;13:2268. https://wwwnature.53yu.com/articles/s41467-022-29915-z.
22 Xia ZL, Sacco M, Hu YM, Ma C, Meng XZ, Zhang FS, Szeto T, Xiang Y, Chen Y, Wang J. Rational design of hybrid SARS-CoV-2 main protease inhibitors guided by the superimposed cocrystal structures with the peptidomimetic inhibitors GC-376, telaprevir, and boceprevir. *ACS Pharmacol. Transl. Sci.* 2021;4:1408–1421.
23 Qiao JX, Li YS, Zeng R, et al. SARS-CoV-2 Mpro inhibitors with antiviral activity in a transgenic mouse model. *Science*. 2021;371:1374–1378. https://doi.org/10.1126/science.abf1611.
24 Owen DR, Allerton CMN, Anderson AS, et al. An oral SARS-CoV-2 Mpro inhibitor clinical candidate for the treatment of COVID-19. *Science*. 2021;374:1586–1593. https://doi.org/10.1126/science.abl4784.
25 Zhao Y, Fang C, Zhang Q, et al. Crystal structure of SARS-CoV-2 main protease in complex with protease inhibitor PF-07321332. *Protein Cell*. 2022;13:689–693. https://doi.org/10.1007/s13238-021-00883-2.
26 Gabriele LM, Alessia B, Antonino L, Martorana A. Targeting SARS-CoV-2 main protease for treatment of COVID-19: covalent inhibitors structure-activity relationship insights and evolution perspectives. *J Med Chem*. 2022;65:12500–12534. https://doi.org/10.1021/acs. jmedchem.2c01005.
27 Ma CL, Sacco MD, Hurst B, et al. Boceprevir, GC-376, and calpain inhibitors II, XII inhibit SARS-CoV-2 viral replication by targeting the viral main protease. *Cell Res*. 2020;30:678–692. https://www.nature.com/articles/s41422-020-0356-z.
28 Konno S, Kobayashi K, Senda M, et al. 3CL protease inhibitors with an electrophilic arylketone moiety as anti-SARS-CoV–2 agents. *J Med Chem*. 2022;65:2926–2939. https://doi.org/10.1021/acs.jmedchem.1c00665.
29 Fu LF, Ye F, Feng Y, et al. Both Boceprevir and GC376 efficaciously inhibit SARS-CoV-2 by targeting its main protease. *Nat Commun*. 2020;11:4417. https://www.nature.com/articles/s41467-020-18233-x.
30 Kneller DW, Galanie S, Phillips G, O'Neill HM, Coates L, Kovalevsky A. Malleability of the SARS-CoV-2 3CL Mpro active-site cavity facilitates binding of clinical antivirals. *Structure*. 2020;28:1313–1320.e3. https://www.sciencedirect.com/science/article/pii/S0969212620303798.
31 Zhang LL, Lin DZ, Kusov Y, et al. α-ketoamides as broad-spectrum inhibitors of coronavirus and enterovirus replication: structure-based design, synthesis, and activity assessment. *J Med Chem*. 2020;63:4562–4578. https://doi.org/10.1021/acs.jmedchem.9b01828.
32 Bai B, Belovodskiy A, Hena M, et al. Peptidomimetic α-acyloxymethylketone warheads with six-membered lactam P1 glutamine mimic: SARS-CoV-2 3CL protease inhibition, coronavirus antiviral activity, and in vitro biological stability. *J Med Chem*. 2022;65:2905–2925. https://doi.org/10.1021/acs.jmedchem.1c00616.
33 Zhang L, Lin D, Sun X, et al. Crystal structure of SARS-CoV-2 main protease provides a basis for design of improved α-ketoamide inhibitors. *Science*. 2020;368:409–412. https://doi.org/10.1126/science.abb3405.
34 Thanigaimalai P, Konno S, Yamamoto T, et al. Design, synthesis, and biological evaluation of novel dipeptide-type SARS-CoV 3CL protease inhibitors: structure-activity relationship study. *Eur J Med Chem*. 2013;65:436–447. https://doi.org/10.1016/j.ejmech.2013.05.005.
35 Ramos-Guzmán CA, Ruiz-Pernía JJ, Tuñón I. Computational simulations on the binding and reactivity of a nitrile inhibitor of the SARS-CoV-2 main protease. *Chem Commun*. 2021;57:9096–9099. https://doi.org/10.1039/D1CC03953A.
36 Ngo ST, Nguyen TH, Tung NT, Mai BK. Insights into the binding and covalent inhibition mechanism of PF-07321332 to SARS-CoV-2 Mpro. *RSC Adv*. 2022;12:3729–3737. https://doi.org/10.1039/D1RA08752E.